Acquisition and processing of topo-bathymetric lidar for Isle Madame in support of the World Class Tanker Safety Initiative

Prepared by

Tim Webster, PhD
Kevin McGuigan, Nathan Crowell,
Kate Collins, Candace MacDonald
Applied Geomatics Research Group
NSCC, Middleton
Tel. 902 825 5475
email: tim.webster@nscc.ca

Submitted to

Fisheries and Oceans Canada

March 15, 2015

How to cite this work and report:

Webster, T., McGuigan, K., Crowell, N., Collins, K., MacDonald, C. 2014. Acquisition and processing of topo-bathymetric lidar for Isle Madame in support of the World Class Tanker Safety Initiative, Applied Geomatics Research Group, NSCC Middleton, NS.

Executive Summary

An airborne topographic-bathymetric lidar survey was undertaken at Isle Madame, Nova Scotia on September 27, 2014. The sensor used was a Chiroptera II integrated topographic-bathymetric lidar sensor equipped with a 60 megapixel multispectral camera. Strong winds in the Maritimes during the week of the planned survey reduced water clarity and delayed the surveys, but eventually the winds died down enough so that good data were collected for the study site. The aircraft required ground-based high precision GPS data to be collected during the lidar survey in order to provide accurate positional data for the aircraft trajectory. The CANSEL active control network was utilized and a GPS base station in Port Hawkesbury was used for the aircraft trajectory. A NS high precision monument was used to establish a temporary GPS base station after the survey and RTK GPS check points were collected along the roads for validation of the lidar, indicating a vertical accuracy better than 10 cm. Lidar data were processed in Lidar Survey Studio and classed into ground, water surface, and seabed points and used to produce a Digital Elevation Model (DEM) for the study area. Maps of the reflected green laser amplitude of the seabed and land area was also produced. This map has been used to classify submerged aquatic vegetation as a preliminary map product. The maximum depth achieved with the lidar sensor approximately 6 m although in one area a maximum depth of 10 m was achieved. The aerial photos were orthorectified using the lidar DEM and direct georeferencing information from the aircraft trajectory. The original aerial photos were captured and orthorectified at a resolution of 5 cm and two mosaic data sets built at 5 cm and 20 cm. There were clouds above the aircraft during the survey and some cloud shadow does appear in the orthophotos. Three test sites were used to process the orthophotos and lidar data for coastal habitat classification of shorelines and sensitive areas. These map products have been draped over the DEM to allow them to be visualized in 3-D allowing for an enhanced interpretation of the coastline for emergency response planning. The lidar DEM was used to build a dataset represent the inundation areas at highest astronomical tide (HAT) which corresponded very well to the extent of coastal salt marshes. Preliminary result of the coastal classification are encouraging and provide more detail than the current mapping. A refinement in the scope of the classification is required to ensure the final map product provides sufficient detail for the requirements. A 2 m storm surge level was also added to the HAT to present areas that may be vulnerable to contamination in the event of a spill during a storm event.

Table of Contents

Table of Figures

1 Introduction

The requirement for accurate and detailed information along Nova Scotia's coastal zone is imperative in order to protect existing infrastructure and plan for future development, and to make sound decisions with regard to activities that support economic growth. With the announcement of the government's plan to create a World Class Tanker Safety program through its plan for *Responsible Resource Development* there is a commitment to protect Canada's shoreline and enhance preparedness and identify environmentally sensitive areas. The plan calls for several actions that can be supported by new and innovative geomatics data including: oil spill preparedness by knowing the composition (geological and biological) of the shoreline in more detail than present, map and characterize environmentally sensitive areas, use the near-shore bathymetry to model the local tidal currents, and chart near-shore hazards to navigation. The requirement for accurate and detailed information along Canada's coastal zone is imperative in order to make sound decisions with regard to activities to support economic development and the movement of raw and refined materials. This information is also required in order to protect existing and planning future infrastructure from storm damage as well as protecting our natural shoreline and sensitive areas in the event of an oil spill. A few areas of the coast have been flown with airborne topographic lidar which only surveys the land elevations and does not provide details on the seabed elevation or seabed material (i.e. Eelgrass barren substrate sand or rock). These data have mainly been used for coastal storm surge flood risk studies, many of which have been conducted by the Applied Geomatics Research Group (AGRG) of the Nova Scotia Community College (NSCC) who have many years of experience with lidar technology and mapping. Recently the NSCC has acquired a topo-bathymetric lidar sensor and high resolution aerial camera that is capable of surveying the land elevations and the submerged coastal topography. The ability of an airborne sensor to accurately survey the near shore bathymetry (submerged elevation) offers an opportunity to produce detailed information across the land-sea boundary in an area that has traditionally not been mapped because of the expense and limitations of traditional mapping technologies (air photos on land and boats and echo sounders on the water).

This new topo-bathymetric lidar mapping system, the Chiroptera II, utilizes a near-infrared and green lasers mounted in an aircraft to precisely measure the topography surrounding coastal waters and also sees through the water to measure what is below. The reflection of the laser from the seabed can be used in conjunction with the elevation and vertical structure of the laser reflections. These data can be used to capture the state of the seabed and aquatic vegetation and act as a quantitative baseline prior to any coastal development and prior to any potential spills of contaminants. The lidar sensor is coupled with a high resolution aerial camera (Leica RCD30) which is capable of collecting traditional true colour images (red, green, and blue or RGB) and also a near-infrared (NIR) image which is highly sensitive to the existence of vegetation, such as exposed seaweed in the coastal zone and salt marsh habitat. The ability of the lidar sensor to acquire detailed elevation data on land and continuously into the submarine environment provides information that can be used for coastal risk assessment and support other initiatives such as the development of hydrodynamic models to predict current speeds which are important for pollution spill preparedness. For the intertidal and sub tidal areas this level of

information has never been surveyed before with such sophisticated equipment and provides a rich series of GIS ready data layers for emergency and planning and deployment in case there is a spill.

The study area is the complex set of islands and coastline at Isle Madame, Janvrin Island and Cape Breton Island south of Louisdale (Figure 1).

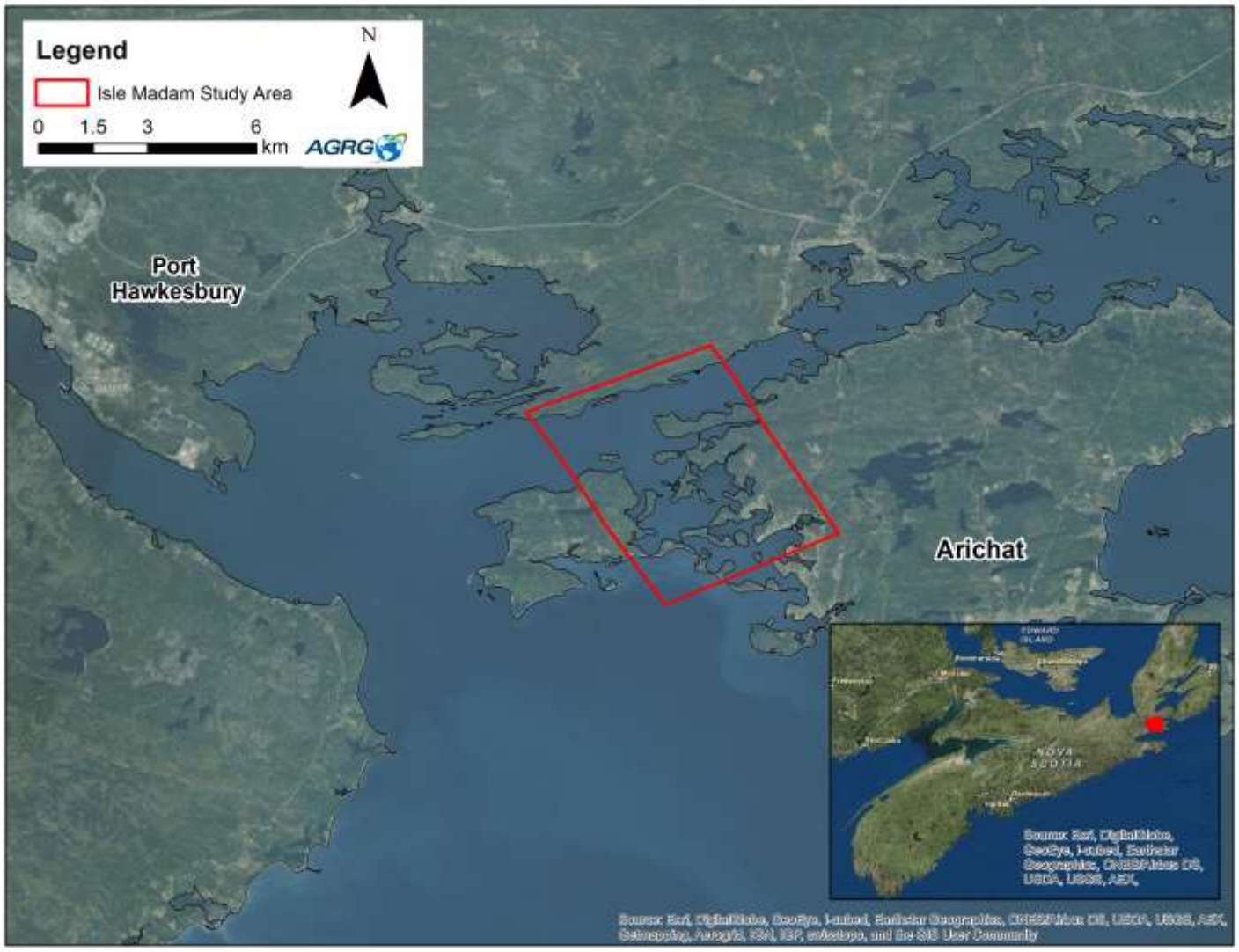

Figure 1 The Isle Madam study area off the coast of Cape Breton Island, Nova Scotia. The coastline is very complex with a series of interconnected land masses.

This report provides information on the instrumentation in the Methods section, including details on the Chiroptera II lidar sensor used for the surveys (Section 2.1) the meteorological conditions during the survey (Section 2.3), and the lidar survey details (Section 2.2). The results include lidar point cloud representations as well as maps of bathymetry, reflectance, and submerged aquatic vegetation coverage, and demonstrations of the coastline classification are found in Section 3.

1.1 Copyright and Data Ownership

The Applied Geomatics Research Group of the Nova Scotia Community College maintains full ownership of all data collected by equipment owned by NSCC and agrees to provide the end user who commissions the data collection a license to use the data for the purpose they were collected for upon written consent by AGRG-NSCC. The end user may make unlimited copies of the data for internal use; derive products from the data, release graphics and hardcopy with the copyright acknowledgement of "Data acquired and processed by the Applied Geomatics Research Group, NSCC". Data acquired using this technology and the intellectual property (IP) associated with processing these data are owned by AGRG/NSCC and data will not be shared without permission of AGRG/NSCC.

2 Methods

2.1 Sensor Specifications and Installation

The lidar used was a Chiroptera II (CH2) integrated topographic bathymetric lidar sensor equipped with a 60 megapixel multispectral camera. The system incorporates a 1064 nm near infrared laser for topographic (topo) laser for ground returns and a green 532 nm laser for hydrographic (hydro) returns (Figure 2). The lasers utilize a Palmer scanner, which forms an elliptical pattern with angles of incidence of 14^{o} forward and back and 20^{o} to the sides of the flight track. This enables more returns, lidar coverage from many different angles, on vertical faces, causes less shadow effects in the data, and is less sensitive to ocean wave interaction. The beam divergence of the topo laser is 0.5 mrad and from the hydro laser (green) is 3 mrad. The topo laser can scan with a pulse repetition frequency up to 400 kHz and the hydro laser can scan with a pulse repetition frequency up to 35 kHz. The hydro laser is limited by depth and water clarity, and has a depth penetration rating of approximately 1.5 x the Secchi depth (a measure of turbidity or water clarity). The Leica RCD30 camera collects co-aligned RGB+NIR motion compensated photographs which can be orthorectified and mosaicked into a single image in post-processing, or analyzed frame by frame for maximum information extraction. The RCD30 is a 60MPIX camera with a focal length lens of 53 mm and produces images 6732 by 9000 pixels in the across and along track direction, respectively. The across track field of view is 54^{o}.

AGRG-NSCC does not own an aircraft, only the sensor, and thus partnered with our Canada Foundation for Innovation project partner, Leading Edge Geomatics (LEG) to assist in the operations of the survey and arranging the aircraft. For the September 2014 field campaign, a twin engine aircraft that was certified to carry the Chiroptera II sensor suite and had a hole suitable to house the sensor head. The main base of operations for the September mission was Fredericton, NB. The aircraft was contracted from Dynamic Aviation in Virginia and arrived in Fredericton on Sunday, Sept. 21. The CH2 sensor also arrived on Sunday with AGRG researchers from Middleton, NS. Staff from Leica Geosystems, who produce the CH2, were delayed in their arrival to Fredericton until late Sunday night.

The sensors were installed in the aircraft on Monday, September 22 (Figure 3a). The aircraft had a hole cut in the bottom for the laser and cameras to image the ground and installation involved fitting the sensor head into the hole (Figure 3c) and the associated control rack on the floor and user display screens on another rack in the aircraft (Figure 3b). Along with the lasers and high resolution camera, the lidar system also includes a 5 megapixel quality assurance camera that the lidar operator is able to view during the flight, along with the waveform of the returning pulse and the flight plan (Figure 3b). Figure 3d shows the downward facing portion of the sensor head, including the red (topographic) and green (bathymetric) lasers, which shoot and return to the large red circles; the lenses on the left and right are the low and high resolution cameras, respectively. During installation the laser systems and camera were calibrated and aligned with the navigation system which consists of a survey grade GPS mounted on the roof of the aircraft and an inertial measurement unit (IMU) mounted above the laser system. Calibration flights were conducted over Fredericton at altitudes of 400 m and 1000 m on Tuesday, Sept. 23, following a wind and rain event on Sept. 22.

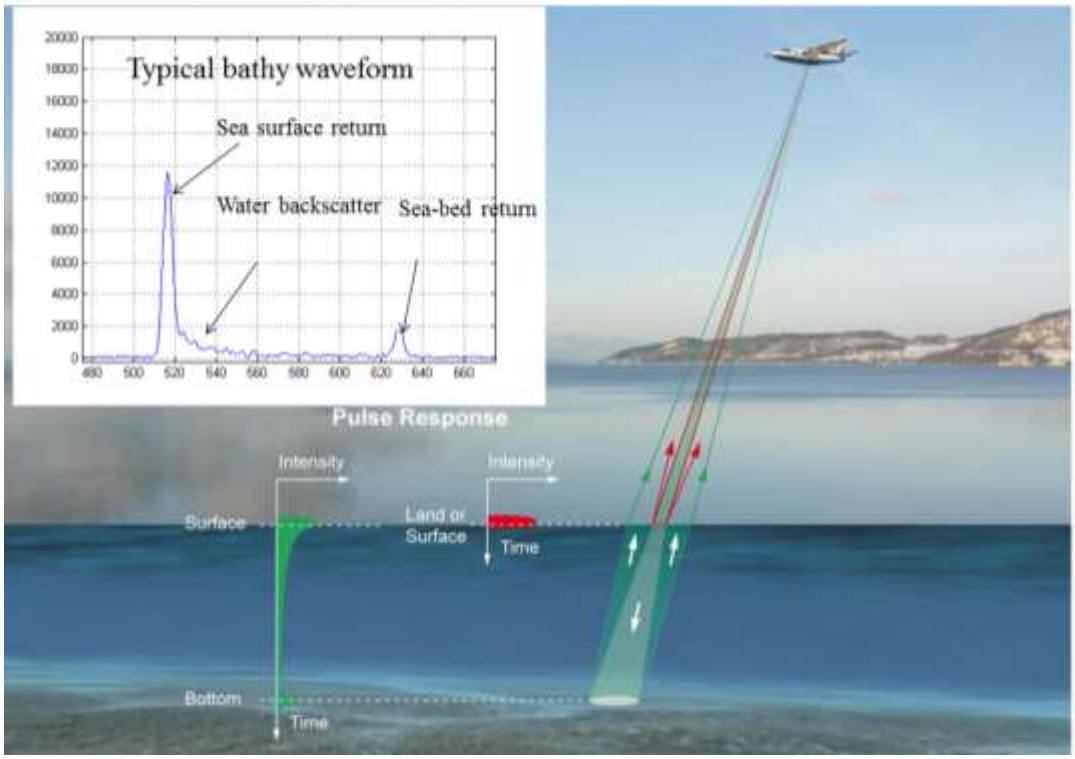

Figure 2 Principles of topo-bathymetric lidar. The system utilizes two lasers: a near infrared and a green laser to surface the land and marine topography.

Figure 3 (a) Aircraft used for September 2014 lidar survey; (b) display monitors on a rack as seen by lidar operator in-flight; (c) main body of sensor control rack (left) and lasers and cameras located over the hole cut in the bottom of the plane (right); (d) large red circles are the lasers; the RCD30 lens (right) and low resolution camera (left) as seen from the bottom of the aircraft.

2.2 Lidar Survey Details

A lidar survey of Isle Madam was conducted on Sept. 27, 2014. The survey was planned using Mission Pro software at an altitude of 400 m above ground at a flying speed of 140 knots. The planned flight lines and photo events are shown in (Figure 4). The study area consisted of a polygon that was approximately 5 km wide by 6.5 km long. The flight lines were planned to cover an area slightly larger than 5 km wide by 8 km long. During the survey several photos were taken of the landscape during the flight (Figure 5).

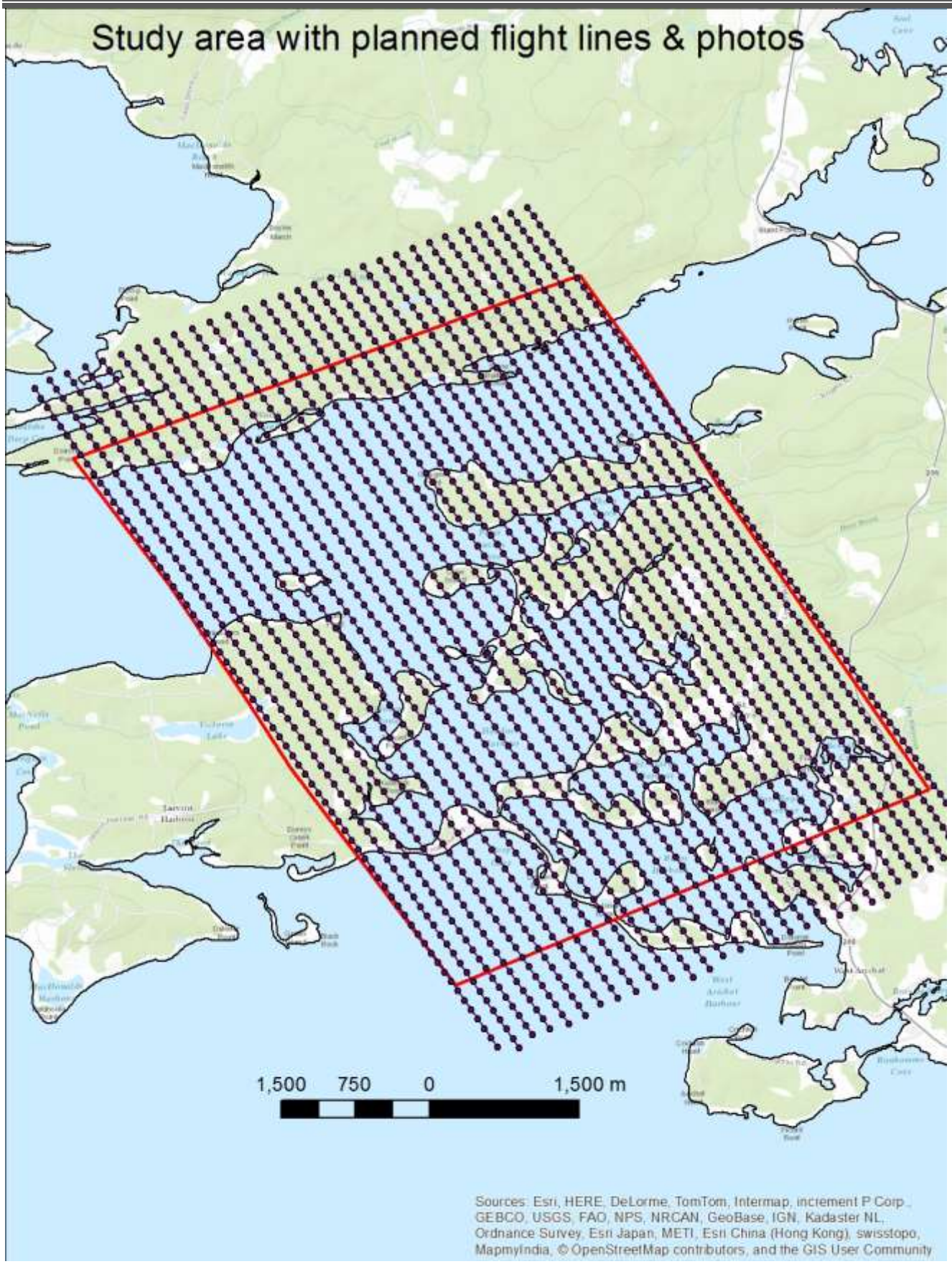

Figure 4 Planned lidar survey flight lines with photo events (dots).

Figure 5 Photographs taken from the plane during the lidar survey showing the complex geographic area of Isle Madam.

2.3 Meteorological Conditions

Meteorological conditions during topo-bathy lidar data collection are an important factor in successful data collection. As the lidar sensor is limited by water clarity, windy weather that stirs up sediment in the seawater can prevent good laser penetration. Rainy weather is not suitable for lidar collection, and the glare of the sun must also be factored in for aerial photography. We used data from Environment Canada's weather station located at Port Hawkesbury (Figure 6) to check on weather conditions at the study area in advance of the lidar survey, and in lidar data post-processing, to assess the meteorological impact on the data. Figure 7 shows meteorological data at Port Hawkesbury for Sept. 14 to 28 and shows a storm event on Sept. 22, with 50 km/h winds blowing from the south. Wind on the days preceding and during the lidar survey on Sept. 27 were between 10 and 20 km/h and blowing mainly from the west.

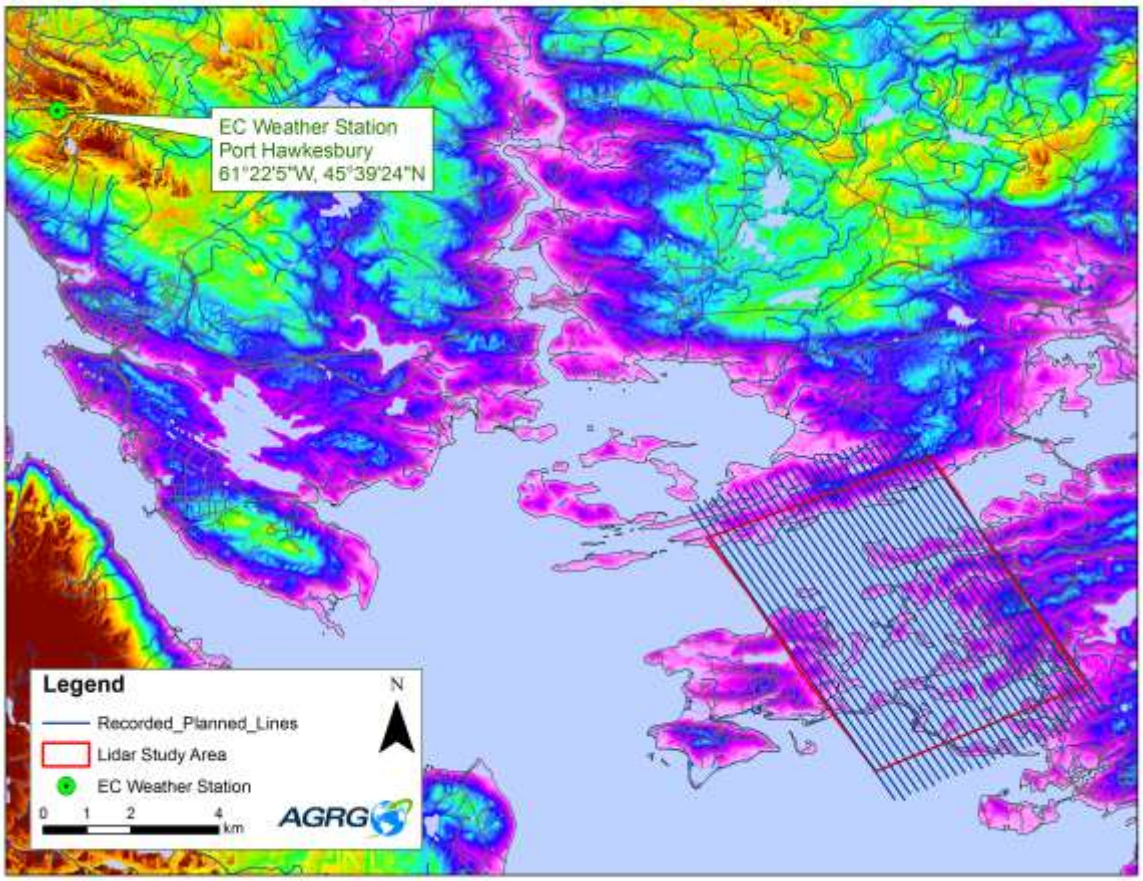

Figure 6 Environment Canada weather station at Port Hawkesbury, NS and lidar study area showing flight lines. Background is the elevation based on a NS 20 m elevation model.

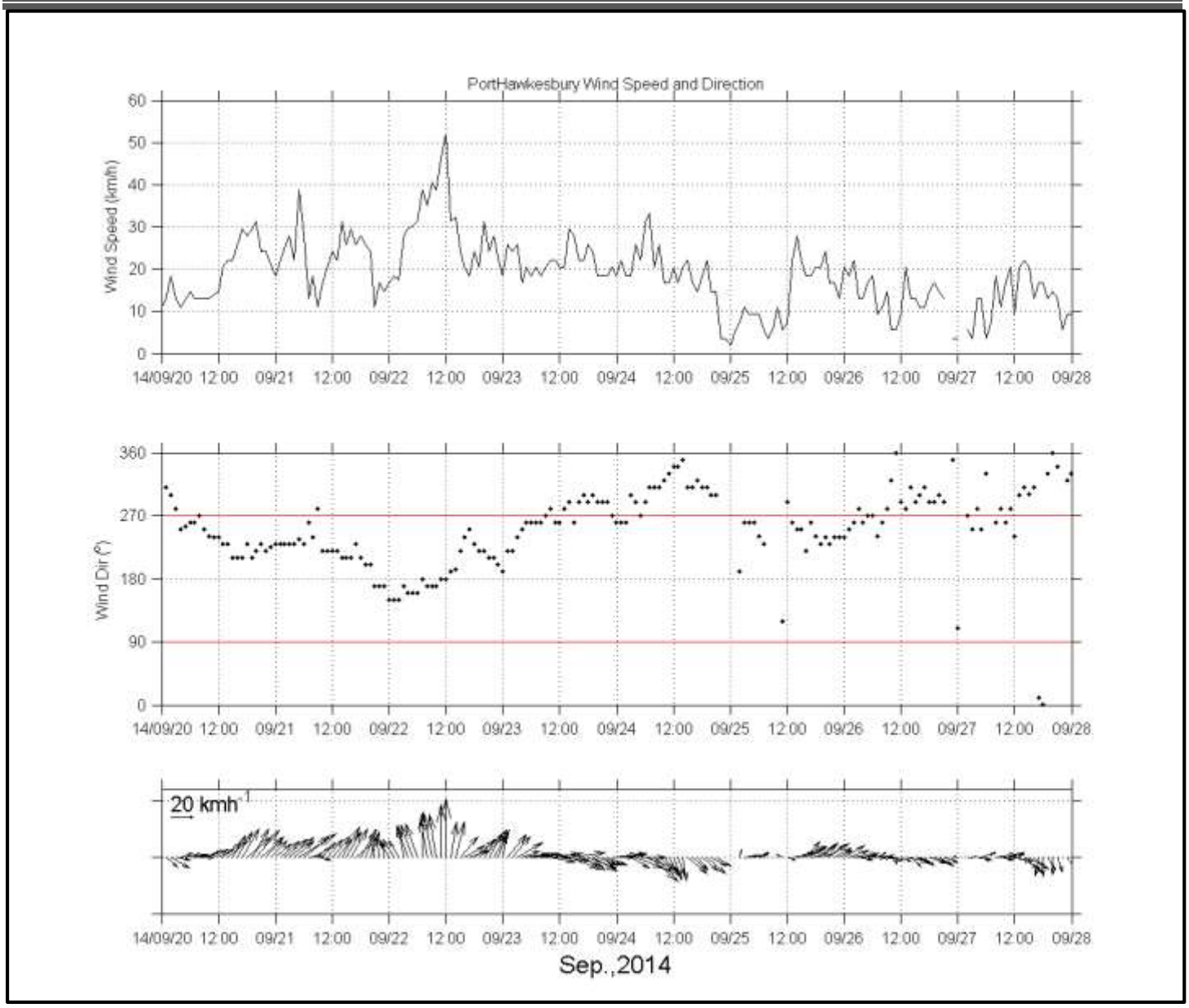

Figure 7 Wind speed (top panel) and direction (middle panel, where the wind is blowing from the direction shown) from Environment Canada weather station at Port Hawkesbury, NS. The lower panel shows vectors representing the direction the wind is blowing towards. The survey was conducted on Sept. 27 with winds around 20 km/hr to the east and south-east.

2.4 Lidar Data Processing

2.4.1 Point Cloud Processing

Once the GPS trajectory was processed for the aircraft utilizing the base station, aircraft GPS observations and combined with the inertial measurement unit, the trajectory data were linked to the laser returns via the GPS time tag and the lidar data were georeferenced. Lidar Survey Studio (LSS) software accompanies the Chiroptera II sensor and is used to process the lidar waveforms into discrete points. The lidar points can be inspected to ensure that the entire study area was captured. One critical step in the processing of bathymetric lidar is the ability to map the water surface. The position of

the water surface is critical for calculating the refraction of the emitted laser pulse and the change in the speed of light in water compared to air. These calculations are necessary to accurately position the laser returns. The LSS software computes the water surface from the lidar returns of both the topo and hydro lasers. In addition to classifying points as land, water surface or bathymetry, the system also computes a water surface that ensures the entire area of water is covered regardless of the original lidar point density. As mentioned, part of the processing involves converting the raw waveform lidar return time series into discrete classified points using LSS signal processing; points include ground, water surface, seabed, etc. Waveform processing may include algorithms specifically for classifying the seabed through high turbidity water columns, where required. The points can be examined in LSS both in plan view and in cross-section view. The waveforms can be queried for each point so that the location of the waveform peak can be identified and the type of point defined, for example water surface and bathymetry; the 5MPIX image associated with the lidar points can be accessed as well to aid in processing. Classified points are analyzed and further refined and filtered to reduce noise and eventually converted into a raster surface at a 2 m spatial sampling interval using ArcGIS. Various grids can then be constructed from the lidar classes and attributes including reflectance and elevation. Examples of the gridded surface models from the HD laser include the seabed reflectance (Figure 8) and the digital elevation model (DEM) (Figure 9). The DEM is actually a hybrid of the topo laser on land and the hydro laser for the submerged terrain. The noise has not been removed on these initial data products as seen in figures 8 and 9.

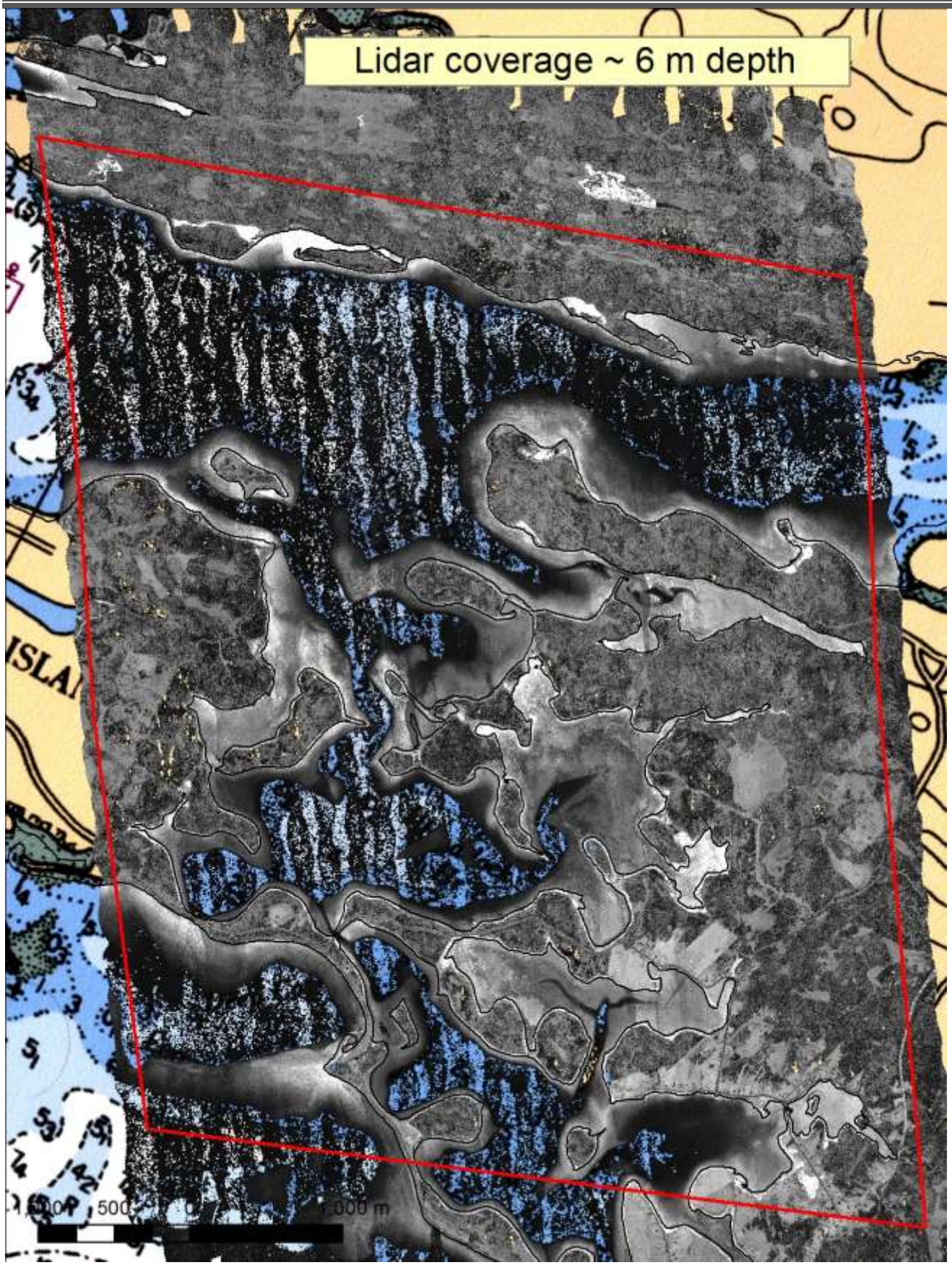

Figure 8 Example of the green laser raw reflectance image overlaid on a CHS chart of the area.

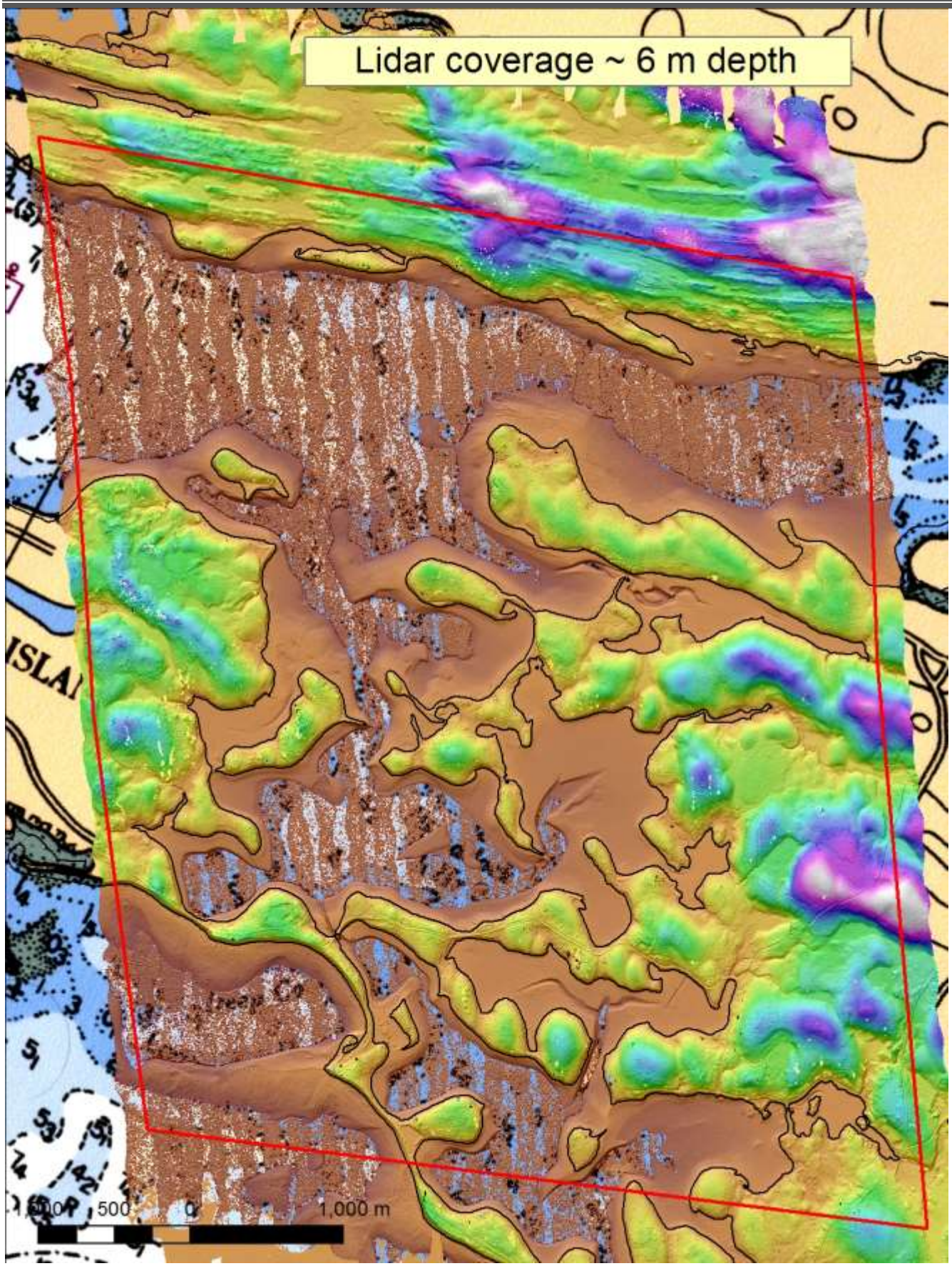

Figure 9 Example of the bare-earth seamless digital elevation model of the land and bathymetry over the chart.

Terrascan was utilized to further classify and filter the lidar point cloud. Because of the differences in the lidar footprint between the TD and HD sensors it was decided that the HD lidar point returns would be used to represent the ocean surface and bathymetry points and the TD lidar points would be used to represent targets above ground. The total point cloud that utilized both sensors was processed in Terrascan where the ground was classified and erroneous points both above and below the ground were defined.

The standard classification numbers used in the LAS format 1.2 do not adequately represent the bathymetric and water surface information, therefore a translation had to be used for the final point cloud. The overlap between flight lines also presented some challenges and it was decided to classify these points separately and code them such that the end user can decide if they want to utilize these points in the surface model construction by coding them uniquely. See **Table 1** for the classification codes.

2.4.1 Gridded Surface Models

There were three main data products derived from the lidar point cloud. The first two were based on the elevation and include the Digital Surface Model (DSM) which incorporates valid lidar returns from vegetation, buildings, ground and bathymetry returns, and the Digital Elevation Model (DEM) which incorporates ground returns above and below the water line. The third data product was the intensity of the lidar returns, or the reflectance of the hydro lidar. The lidar reflectance, or the amplitude of the returning signal from the hydro laser, was influenced by several factors including water depth, the local angle of incidence with the target, the natural reflectivity of the target material, and the voltage or gain of the transmitted lidar pulse. The original data was difficult to interpret because of variances as a result of water depth and loss of signal due to the attenuation of the laser pulse through the water column at different scan angles. The reflectance values were normalized by taking samples of the reflectance values of a common cover type, such as sand, over depth ranges and using these data to establish a relationship between depth and the logarithm of the reflectance value; the inverse of this relationship was used to normalize the data. To compensate for the loss of the green laser pulse signal through attenuation in the water column and allows for more qualitative and quantitative analysis of the seabed reflectance (Figure 10). These data were examined and a preliminary classification of submerged vegetation was conducted from the depth normalized reflectance. This is an area of active research and we expect to improve the level of accuracy and detail as this project progresses.

Class number	Description
0	Water model
1	Bathymetry (Bathy)
2	Bathy Vegetation
3	N/A
4	Topo laser (TD) Ground
5	TD non-ground (vegetation & buildings)
6	Hydro laser (HD) Ground
7	HD non-ground
8	Water
9	Noise
10	Overlap Water Model
11	Overlap Bathy
12	Overlap Bathy Veg
13	N/A
14	Overlap TD Ground
15	Overlap TD Veg
16	Overlap HD Ground
17	Overlap HD Veg
18	Overlap Water
19	Overlap Noise

Table 1 Table of delivered LAS classes combining the hydro (HD) and topo (TD) lidars.

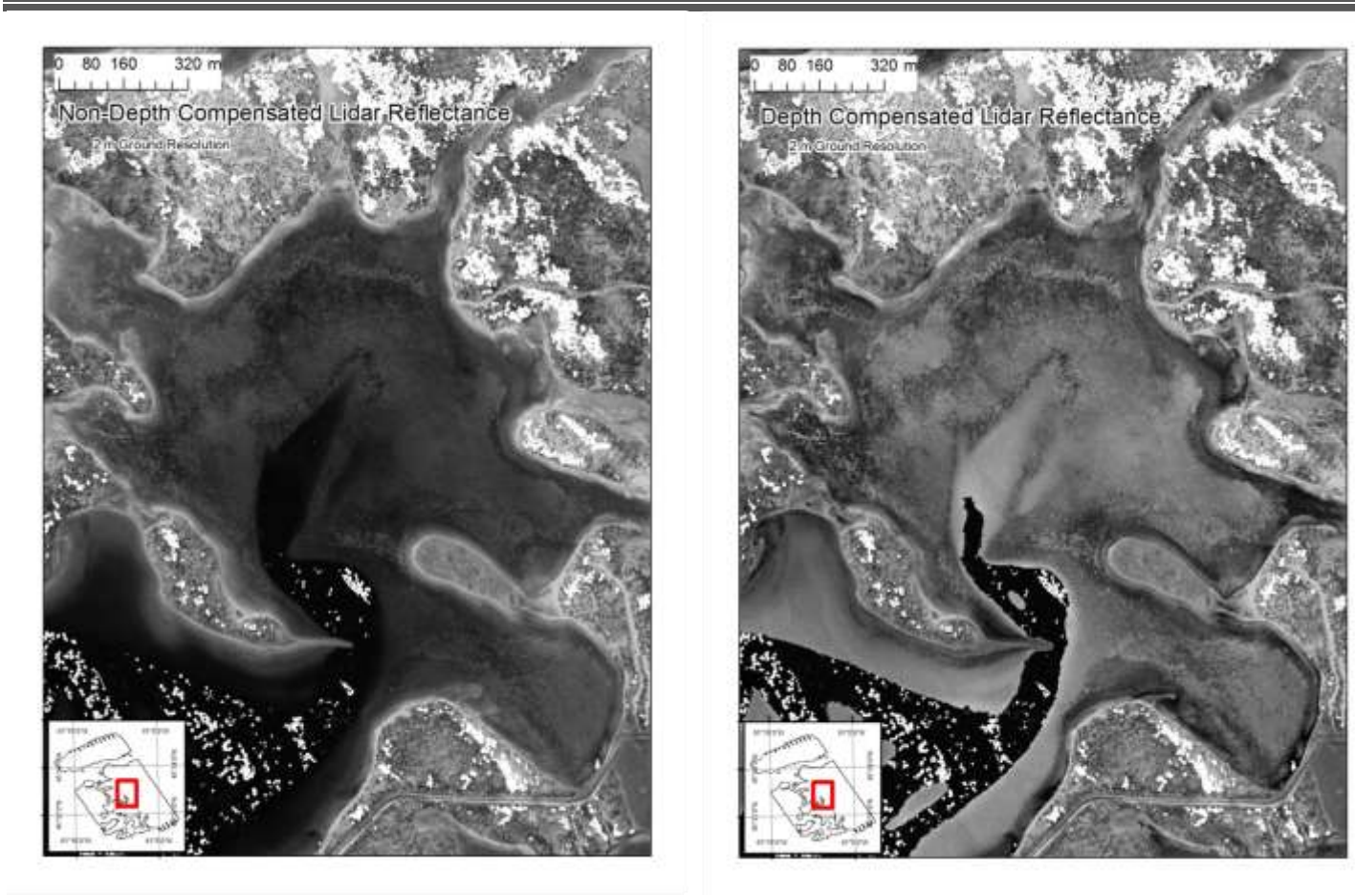

Figure 10 Example of the original reflectance from the green laser of the seabed (left map) compared to the depth normalized reflectance (right map).

The elevation of the lidar point cloud is relative to the WGS84 ellipsoid since the points were geolocated based on the GPS aircraft trajectory. The geoid-ellipsoid separation model, HT2, from Natural Resources Canada, was used to convert the DSM and DEM surface models to orthometric heights referenced to the Canadian Geodetic Vertical Datum of 1928 (CGVD28). In addition to the conversation of elevations from ellipsoidal heights to orthometric heights, the noise has been removed from the dataset so only legitimate elevations are represented (Figure 11).

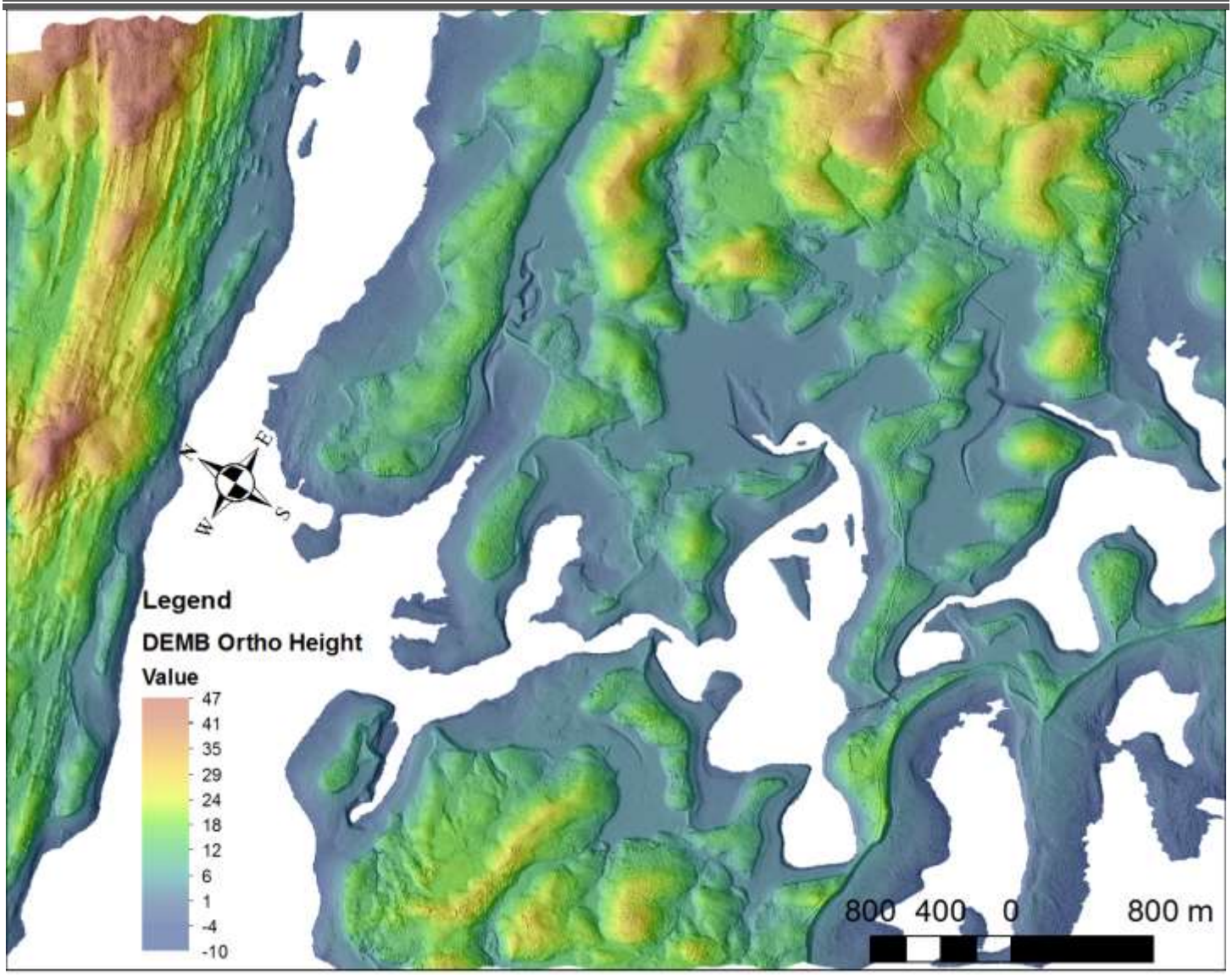

Figure 11 Example of the cleaned seamless DEM orthometric elevations referenced to CGVD28. Note the north arrow and that the map has been rotated so the top is northeast.

2.4.2 Aerial Photo Processing

The RCD30 60 MPIX imagery was processed using the aircraft trajectory and direct georeferencing. The setup effectively recorded multispectral RGB-NIR imagery (blue 470 nm, green 530 nm, red 590 nm, NIR 780 – 900 nm) at 5 cm ground pixel resolution. Photo events were planned and collected within the Leica MissonPro software package. A full coverage was planned and achieved without slivered data or missing frames for the entirety of the Isle Madame study area. Photos were developed from raw "DarkFrames" to 4 band TIF files within the Leica FramePro software package. Standard Leica radiometric calibrations were applied to each frame in addition to atmospheric corrections (Colour Saturation = 1.8; Gamma = 1.8; Gain = 4) and the four 8 bit image bands were generated (RGB-NIR) (Figure 12).

Figure 12 Example of RGB image on the left and grey scale near infrared band on right.

The low altitude and high resolution of the imagery required that the lidar data be processed first to produce bare-earth digital elevation models (DEMs) that were used in the orthorectification process. The aircraft trajectory, which blends the GPS position and the IMU attitude information into a best estimate of the overall position and orientation of the aircraft during the survey. This trajectory, which is linked to the laser shots and photo events by GPS based time tags, was used to define the Exterior Orientation (EO) for each of the RCD30 aerial photos that were acquired. The EO, which has traditionally been calculated by selecting ground control point (x,y, and z) locations relative to the air photo frame and calculating a bundle adjustment, was calculated using direct georeferencing and exploiting the high precision of the navigation system. The EO file defines the camera position (x,y,z) for every exposure as well as the various rotation angles about the x,y and z axis known as omega, phi and kappa. The EO file along with a DEM can be used with the aerial photo to produce a digital orthophoto. Initially, processing was attempted to produce the orthophotos without the lidar DEM. This resulted in orthophotos from adjacent frames not lining up. After the lidar data were processed and classified into ground points, the lidar-derived DEM (above and below the water line) was used in the orthorectification process in Erdas Imagine software and satisfactory results were produced. The photos show a high level of detail where direct measurements can be extracted including boat launches and other critical infrastructure that may be of interest during a spill cleanup (Figure 13).

Figure 13 Example of RCD30 orthophoto 5 cm mosaic where measurements of boat launch sites can be made directly from the orthophoto.

2.4.3 Lidar Validation

Survey grade GPS checkpoints were collected to compare to the lidar points and surface models to ensure the vertical accuracy of the data was sufficient. The GPS elevations were converted from ellipsoidal height to orthometric heights using HT2 within Leica GeoOffice. The GPS antenna was mounted on a vehicle and GPS points were collected along the roads across the study area where the radio signal from the base station could be received. The main set of checkpoints crosses the flight lines in a perpendicular direction which is ideal to test the vertical accuracy of the data. The results of the validation will be shown in the results section. GPS checkpoints over bare ground were overlaid with the lidar DEM and the raster cell values were appended to the point file. The difference in elevation between the GPS point and the lidar derived DEM was then computed and summary statistics calculated. The delta Z values, or DZ, were then displayed graphically on the map showing points within the vertical specifications of 15 cm and those that exceeded it (Figure 14).

As well the histogram of the DZ was displayed and the statistics calculated. The results indicate the mean difference in DZ was -0.06 m with a standard deviation of 0.05 m indicating the data are extremely accurate (Figure 14).

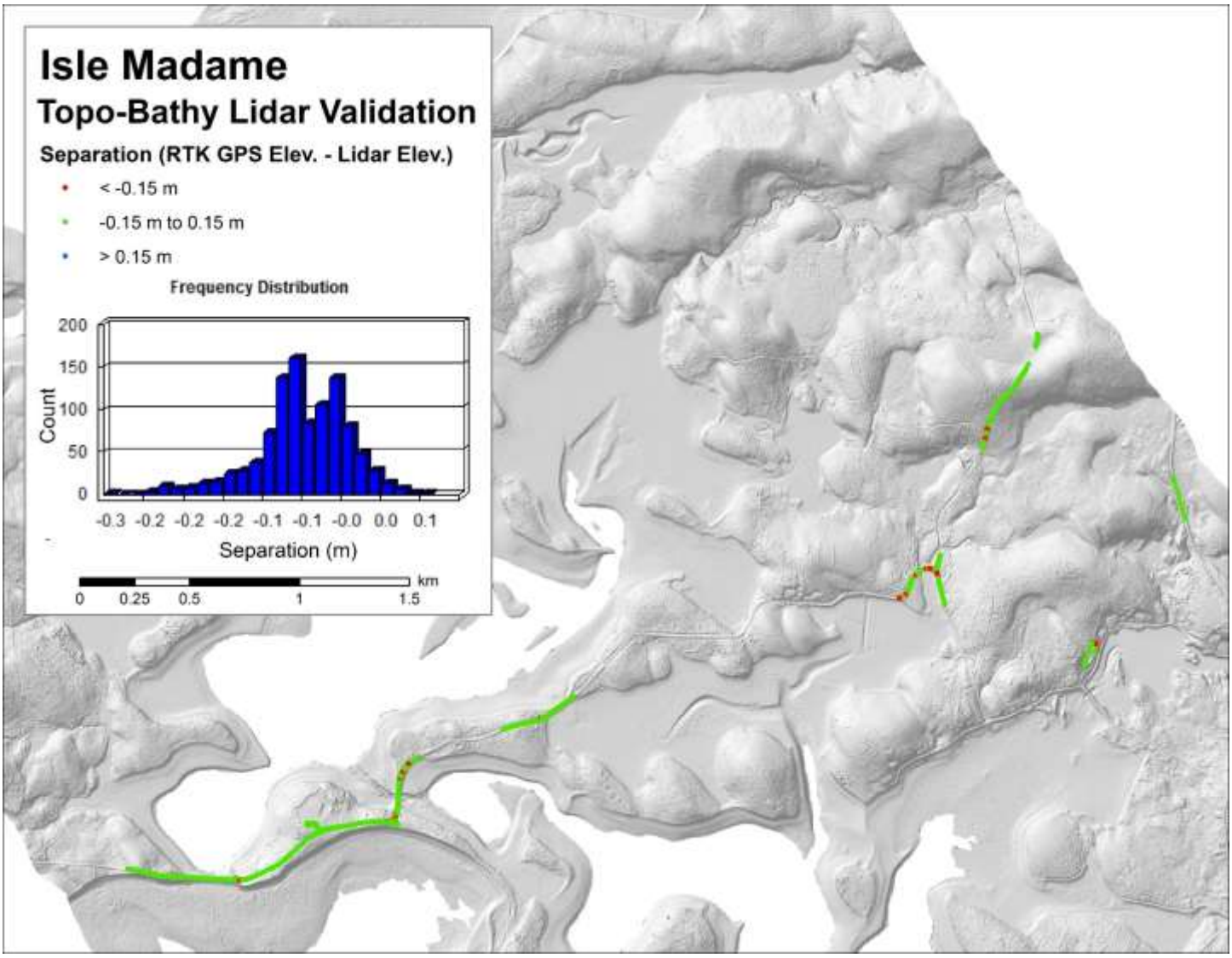

Figure 14 Results of GPS validation of the vertical accuracy of the topographic lidar. The GPS points are colour coded based on the DZ (GPS-DEM) and the histogram of DZ is displayed, mean DZ = -0.06 m, standard deviation DZ = 0.05 m.

2.4.4 Seabed and shoreline classification

In addition to the production of the lidar and orthophto GIS products, we also briefly experimented with the development of the next generation of seabed and shoreline maps to aid in spill cleanup preparation. Three sites were selected to conduct the experiments with the orthophotos and lidar products (Figure 15).

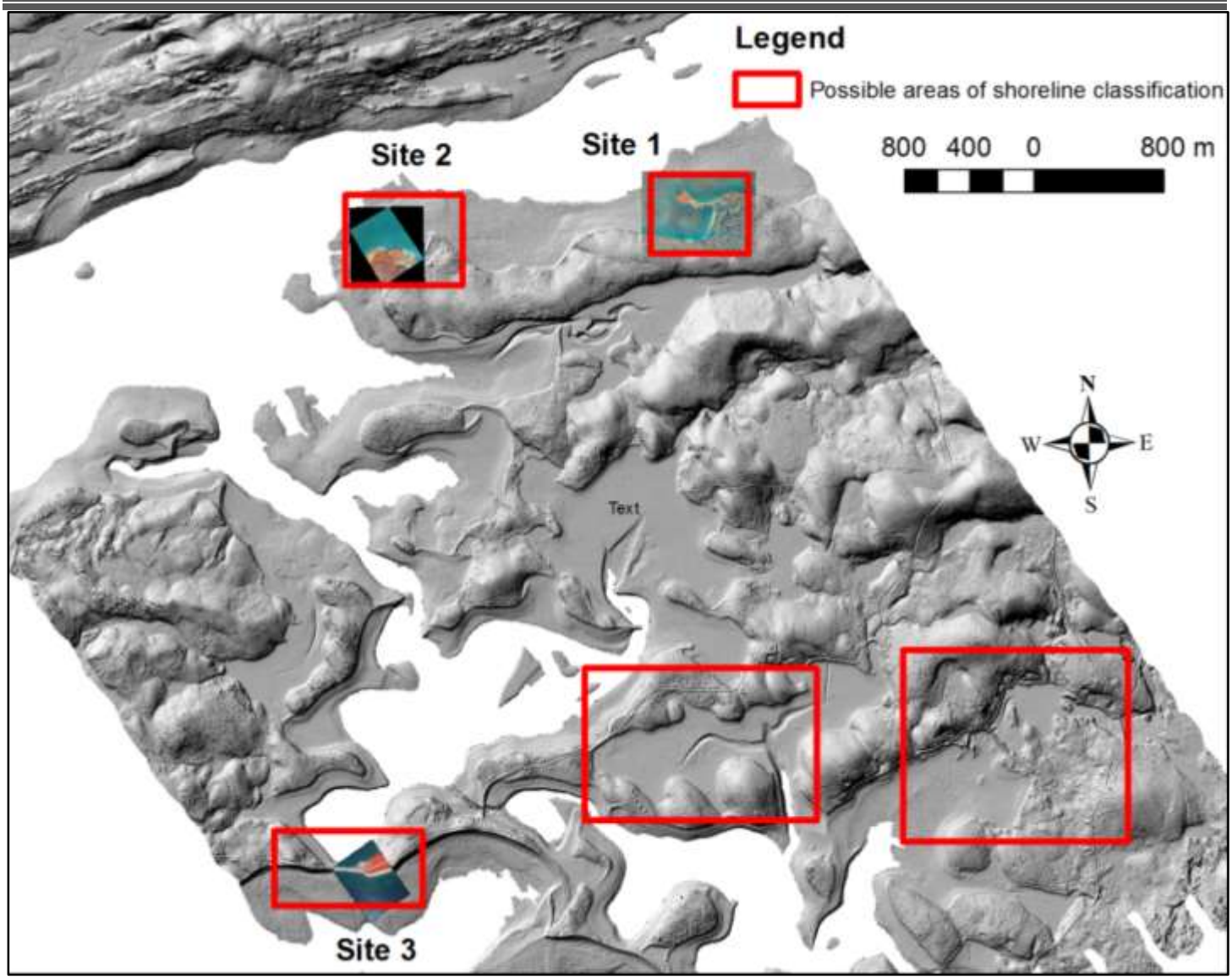

Figure 15 Location of the three test sites where experiments were conducted for shoreline classification.

In addition to the seabed and shoreline classification, the seamless DEM was used to produce a map based on the tidal information from the area. The tidal elevations of the predicted tidal levels from Arichat were used and included: Lowest Astronomical Tide (LAT), the Lower Low Water Large Tide (LLWLT), Mean Water Level (MWL), Higher High Water Large Tide (HHWLT), Highest Astronomical Tide (HAT), and because we are interested in planning for a possible spill which is more likely to occur during stormy weather we also calculated the elevation of HAT plus a 2 m storm surge. The value of 2 m also accounted for possible wave runup if the surge does not reach 2 m which is not common for this region. These values were available from the Canadian Hydrographic Service (CHS) and referenced to the local chart datum which were converted to CGVD28 and projected onto the lidar seamless DEM. This map represents the intertidal area that is potentially vulnerable to spill contamination as well shows the extent of possible inundation inland in the event of a storm surge during the time of the spill (Figure 16). The dark blue on the map represents the maximum depth up to the LAT tidal limit, while the light blue represents the region from LAT to the LLWLT limit (Figure 16).

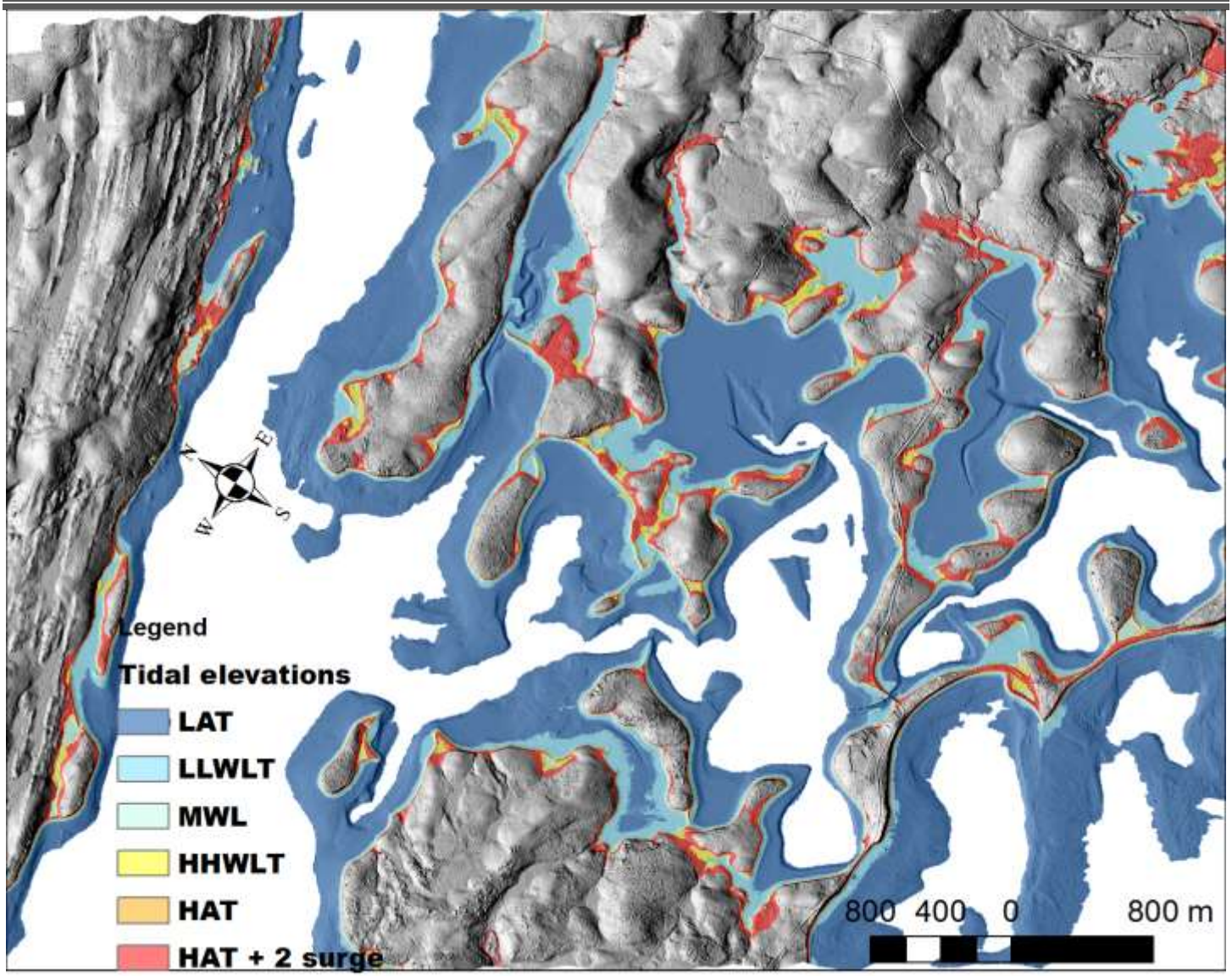

Figure 16 Using the DEM to map the tidal extents plus a 2 m storm surge. The elevation of HAT, for example, is the boundary between the dark blue and light blue polygons.

The classification of the seabed below the waterline during the acquisition of the aerial data was conducted for only one site using the orthophotos and the normalized reflectance data. Additional ground-truth data were required in order to more accurately analyze our results. The result of classifying the seabed based on the orthophotos alone indicated promise where the wave effects and water clarity allowed for a clear image of the seabed (Figure 17). At another site we experimented with using the normalized reflectance of the lidar to map the seabed (Figure 18). This method had two

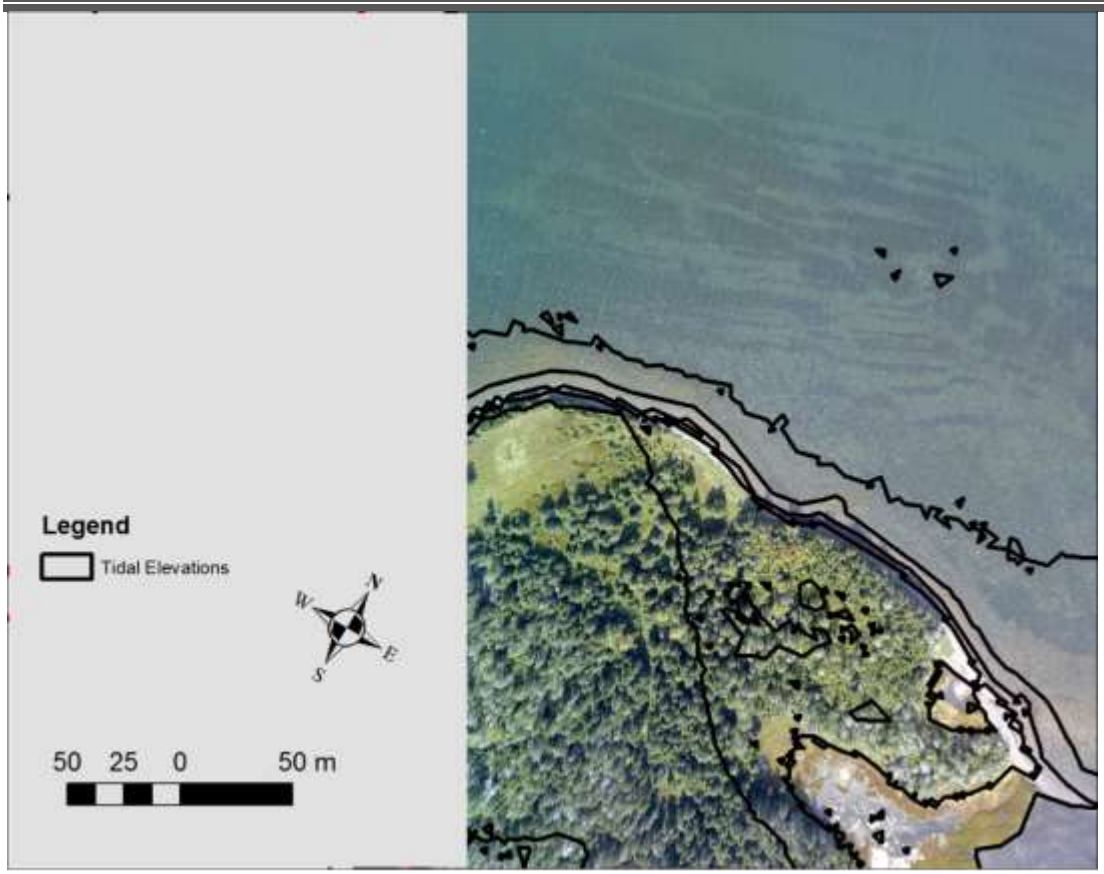

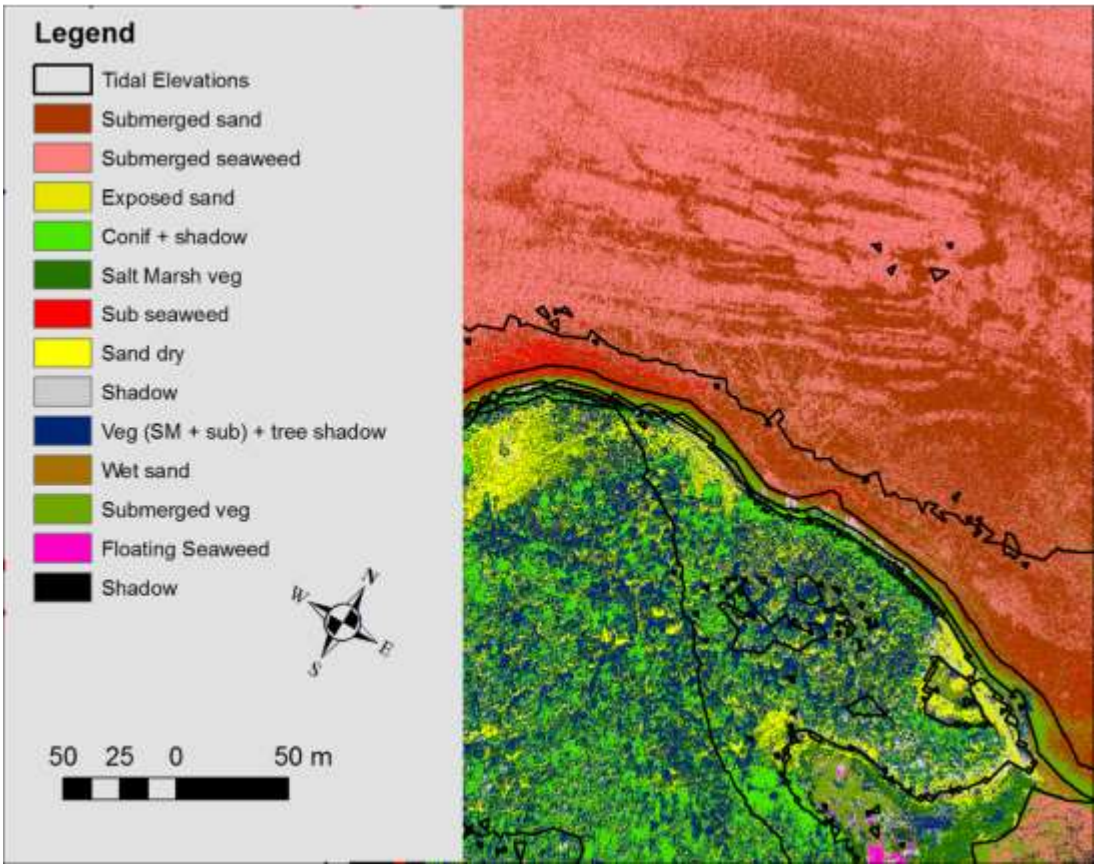

Figure 17 Example of the seabed classification. Top image is a true colour image of the coastline with the tidal elevation vectors. The bottom image shows the results of the classification of the seabed into sand and seaweed (shades of red).

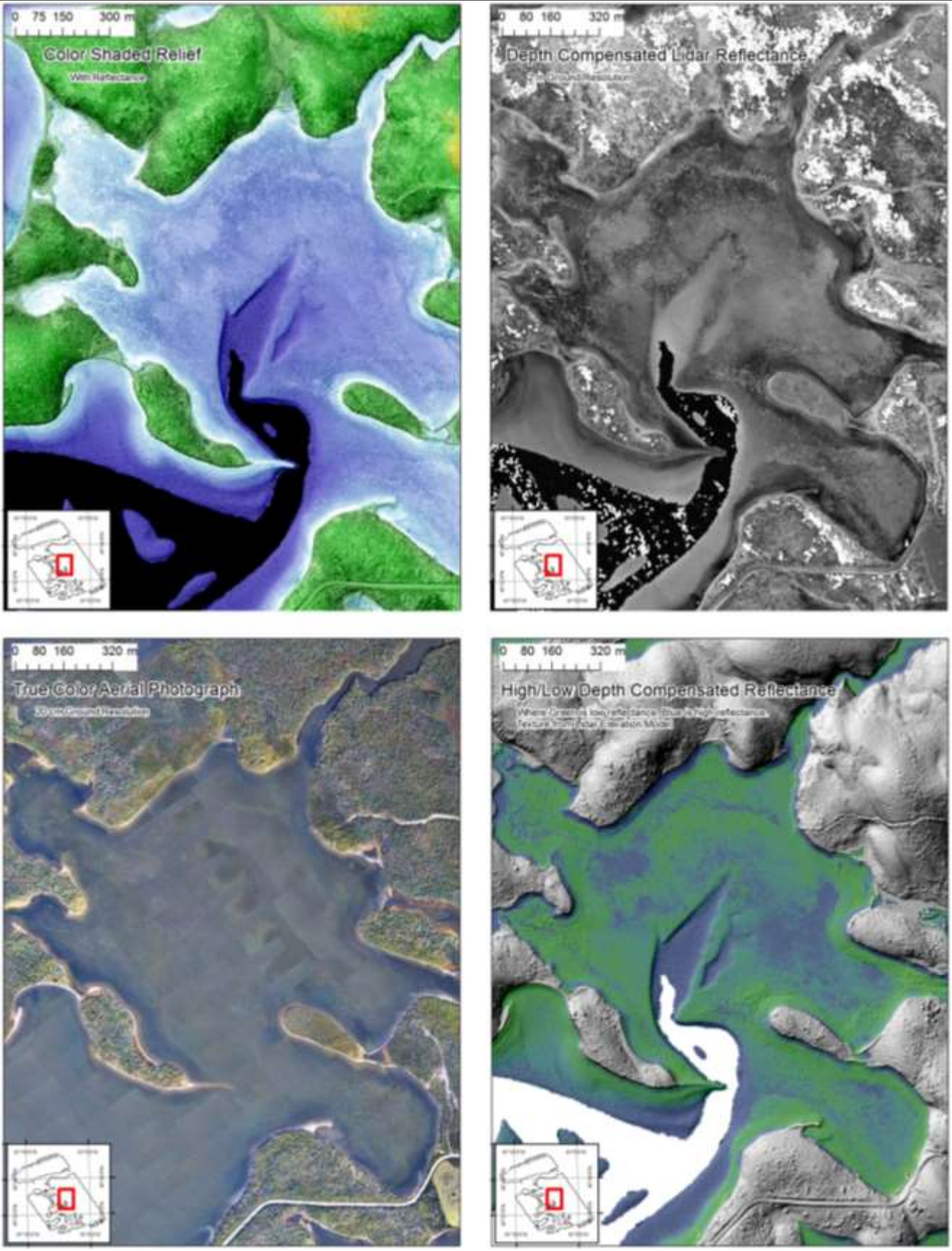

Figure 18 Example of seabed mapping using the normalized lidar reflectance. Top left image is the colour shaded relief map with reflectance. Top right is the normalized reflectance. Lower left is the true colour orthophoto mosaic. Bottom right is the seabed colour coded to represent submerged vegetation (green tones) and sand/rock (blue tones).

advantages to using the orthophotos: 1) if the surface waves do not allow the seabed to be visible, and 2) in addition to the reflectance it also provides insights into the vertical structure of the vegetation. In figure 18 it is difficult to interpret the seabed using the true colour RCD30 imagery, whereas with the reflectance image (Figure 18, top right), the seabed has a high contrast and patterns can easily be followed. This image represents the ground green pulse reflectance or amplitude adjusted for water depth. The white areas on land are regions where no ground points were classified and correspond to dense vegetation (conifer stands) or buildings (Figure 18).

For the shoreline classification two approaches were experimented with: 1) a combination of using the lidar derivatives and the RCD30 orthophoto image bands, and 2) the RCD30 orthophoto imagery. For the various input data, both unsupervised K-means and supervised classification using the maximum likelihood classifier were evaluated. In the case of combining lidar derivatives with RCD30 image bands, experiments were conducted to take advantage of the DEM and DSM as well as the slope derived from the DEM (Figure 19). The RCD30 bands or images were used as well as deriving a Normalized Vegetation Difference Index (NDVI) which highlighted the health or vigor of vegetation. The NDVI was calculated by the difference of the NIR band and the red band divided by the sum of the NIR and red band (Figure 19).

The fact the RCD30 imagery has the combination of visible RGB bands and the NIR band provided a rich set of imagery for coastal applications. The NIR band is very sensitive to vegetation and reflects the energy in this region of the spectrum very strongly. In contrast NIR energy does not penetrate water and thus is very useful in defining the land-water boundary which in some cases can be difficult with visible bands (RGB). The NIR response is also quite different for coniferous vegetation (needle bearing) compared to deciduous (broad leaf) vegetation. In addition to the imagery and lidar being combined for image classification, imagery can be visualized with the terrain models that quickly allows one to interpret the coastal shoreline characteristics in terms of relief, access and vulnerability to contaminants. In the case of low relief coastal areas where salt marshes occur, the RGB and NIR imagery can provide insights into different states of vegetation and relief (Figure 20).

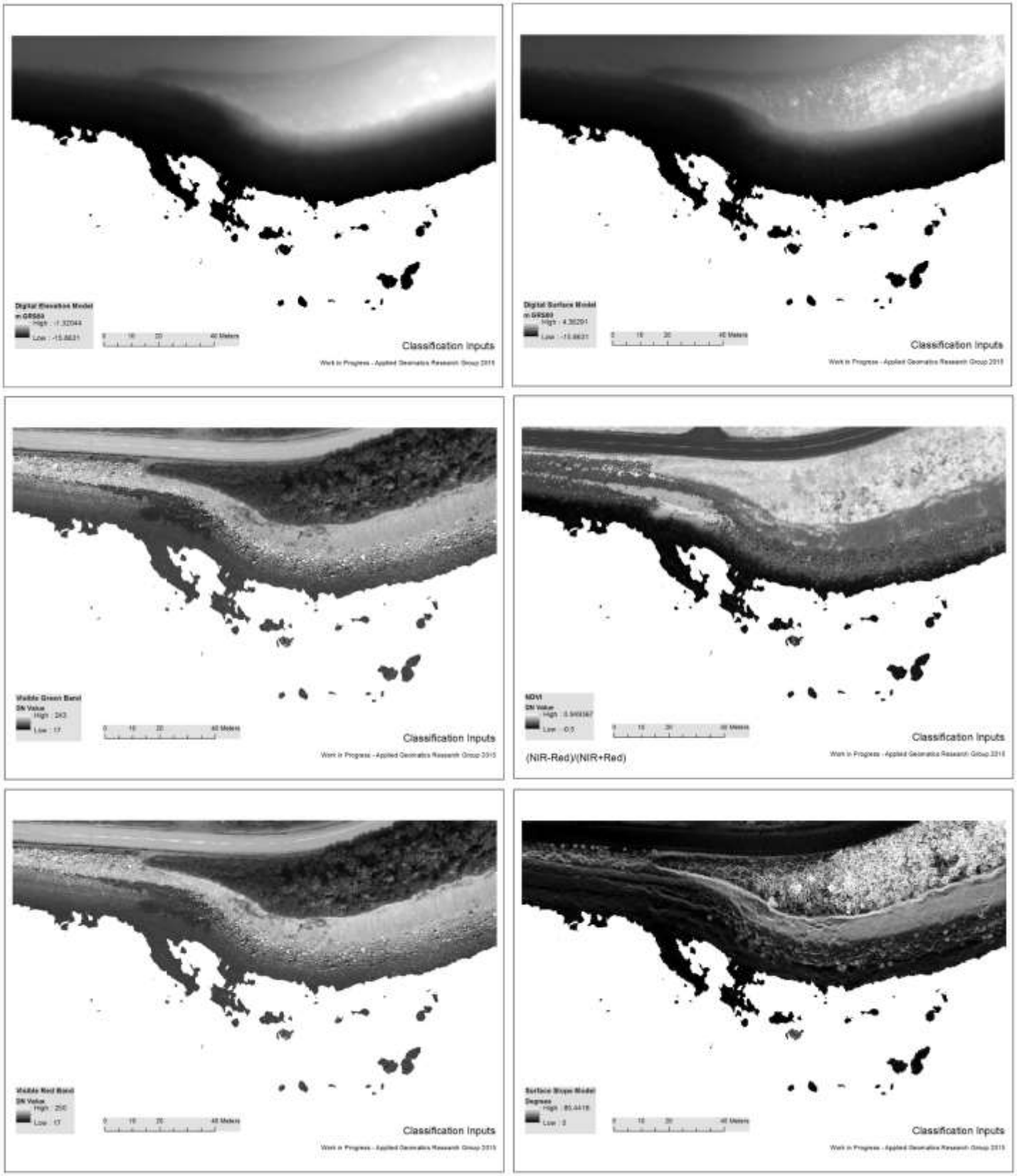

Figure 19 Example of lidar and RCD image inputs for classification of study site 3. Top left lidar DEM, top right lidar DSM, middle left RCD30 green band, middle right RCD30 NDVI, lower left RCD30 red, lower right lidar DEM slope in degrees.

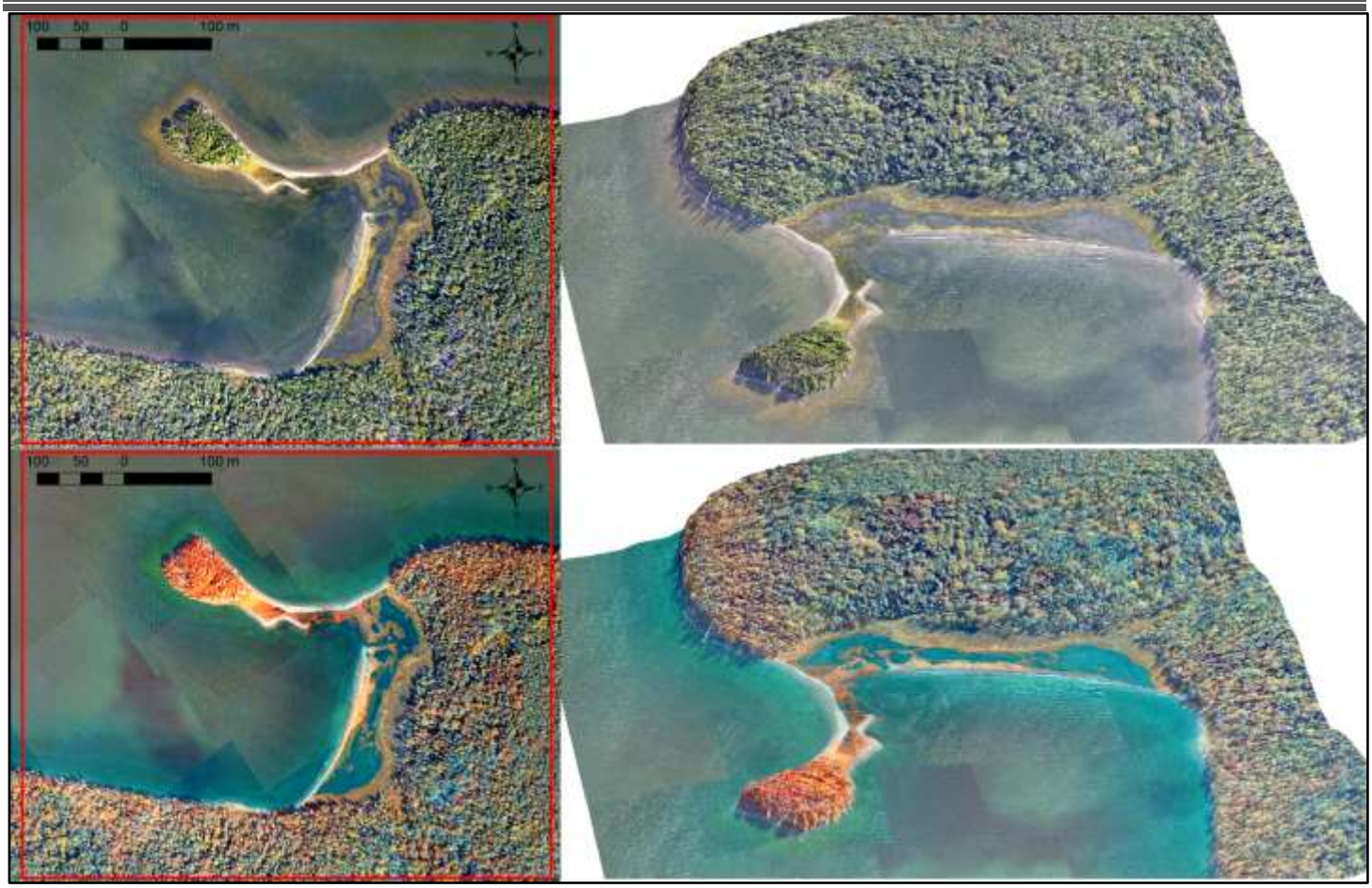

Figure 20 Example of RCD imagery for a coastal salt marsh area, study area 1. Top left is a true colour RGB image, top right is the same image draped over the lidar DEM. Lower left image is a colour NIR image (vegetation in shades of red), lower right is the same image draped over the DEM.

In other coastal areas, it is sometimes difficult to infer the local relief by viewing an orthophoto, where the relief displacement has been removed. The local relief can have significant importance to both the potential of the coastline to be contaminated from a marine based spill as well as access to the coastline for cleanup. The ability to drape the imagery over the DEM is extremely useful to visualize the geographic area in detail without actually visiting the site. For example, the plan view orthophoto for the study site 3 shows a causeway with what appears to be a sand beach to the east (Figure 21). However, once the imagery is draped over the terrain model it becomes clear that the exposed sediment east of the causeway is in fact a steeply sloped glacial till bank while the north side of the coastline is defined by a shallower slope with vegetation occurring down to the waterline where there is infrastructure to allow for launching of a boat (Figure 21). The colour NIR image highlights the vegetation within the area in shades of red. In the perspective view it becomes clear that the vegetation along the sloping glacial till bank represents trees and other material that has fallen from the top, while the dense red patch directly east and south of the causeway represents a patch of seaweed based on its elevation relative to sea-level (Figure 21).

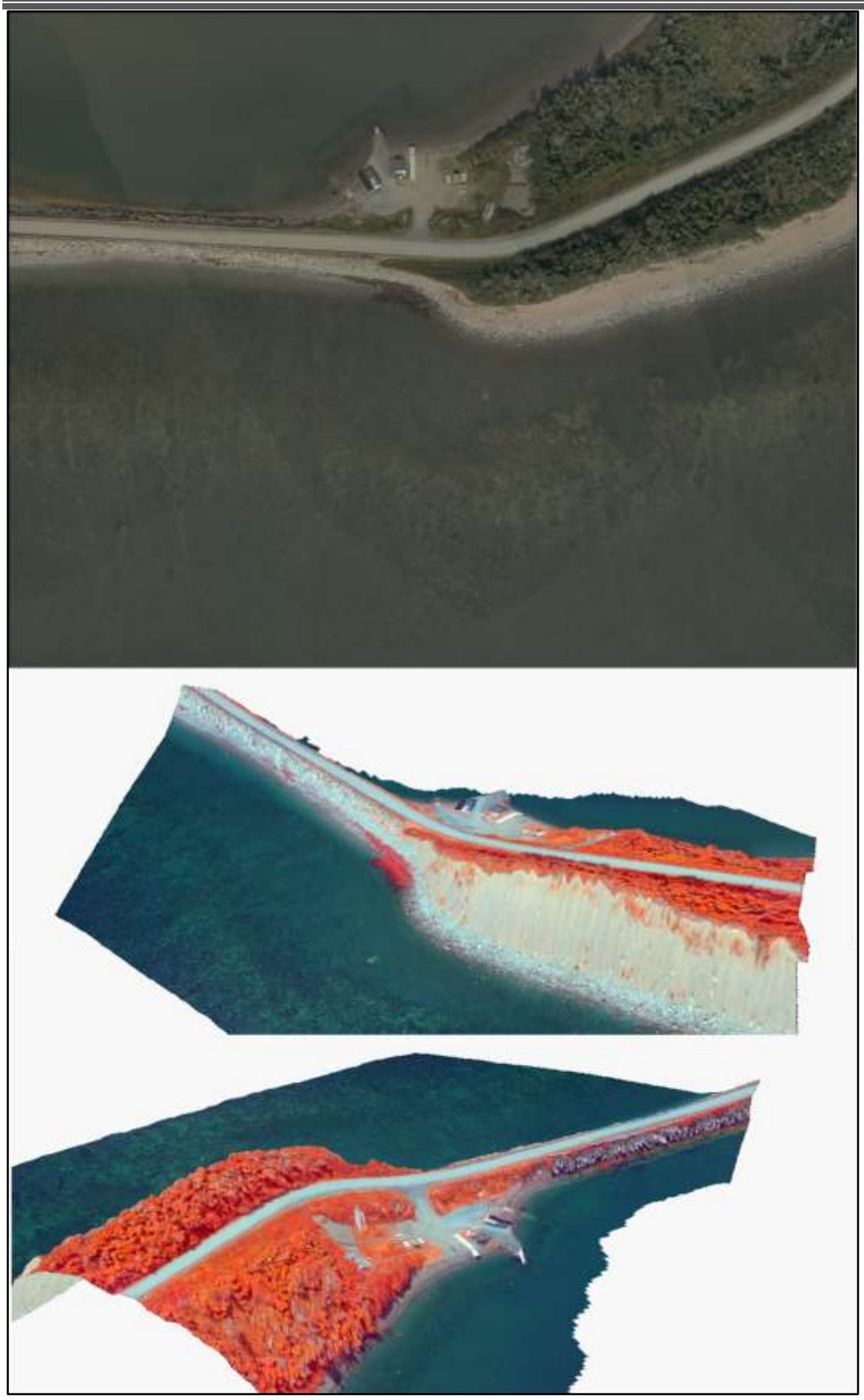

Figure 21 Example of a true colour plan view image (top) and the perspective view, 5 times vertical exaggeration, of the colour NIR image viewed from the south (middle) and from the north (lower) of study site 3.

3 Results

The GPS trajectory information for the aircraft has been processed and used in processing the lidar and aerial photography. A seamless Digital Elevation Model has been constructed from a combination of the topo and hydro laser data (Figure 22) and orthophotos have been processed from the aerial photographs. The lidar reflectance has also been constructed from lidar point data.

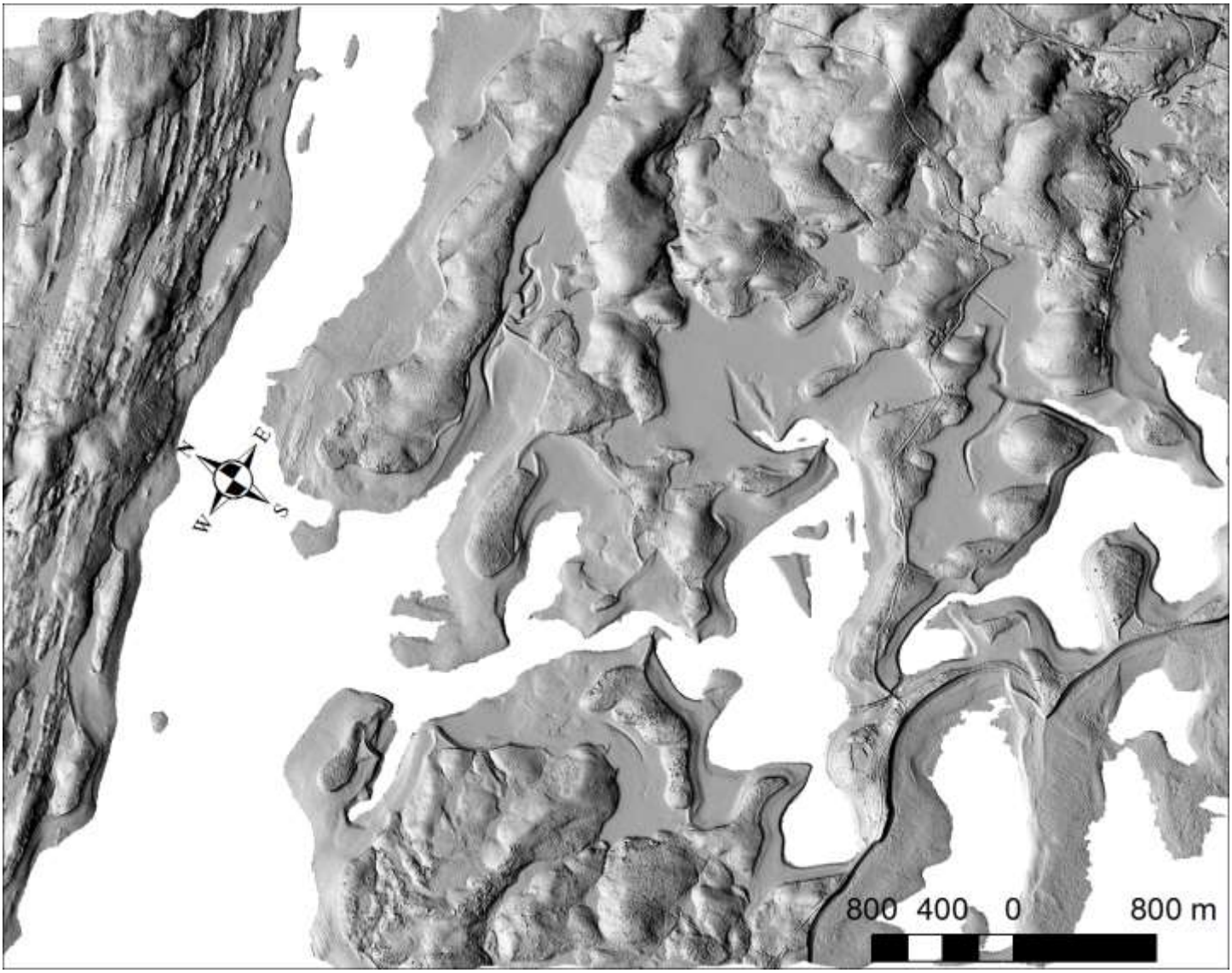

Figure 22 Final shaded relief of the seamless DEM of the study area.

In addition to the lidar and orthophoto products, three areas were used to experiment with the derivation of shoreline classifications using either the RCD30 imagery or the lidar reflectance or a combination of the two. Study site 1 is an example of a sensitive coastal salt marsh area (Figure 15). The DEM was used to construct various tidal elevations including the HHWLT and HAT, which correspond to the extent of the salt marsh vegetation based on the orthophoto interpretation. Thus, this tidal layer can be used to quickly assess where critical salt marsh habitat may exist within the study area (Figure 16). The imagery was used to classify the coastal marsh wetland vegetation into more detail (Figure 23).

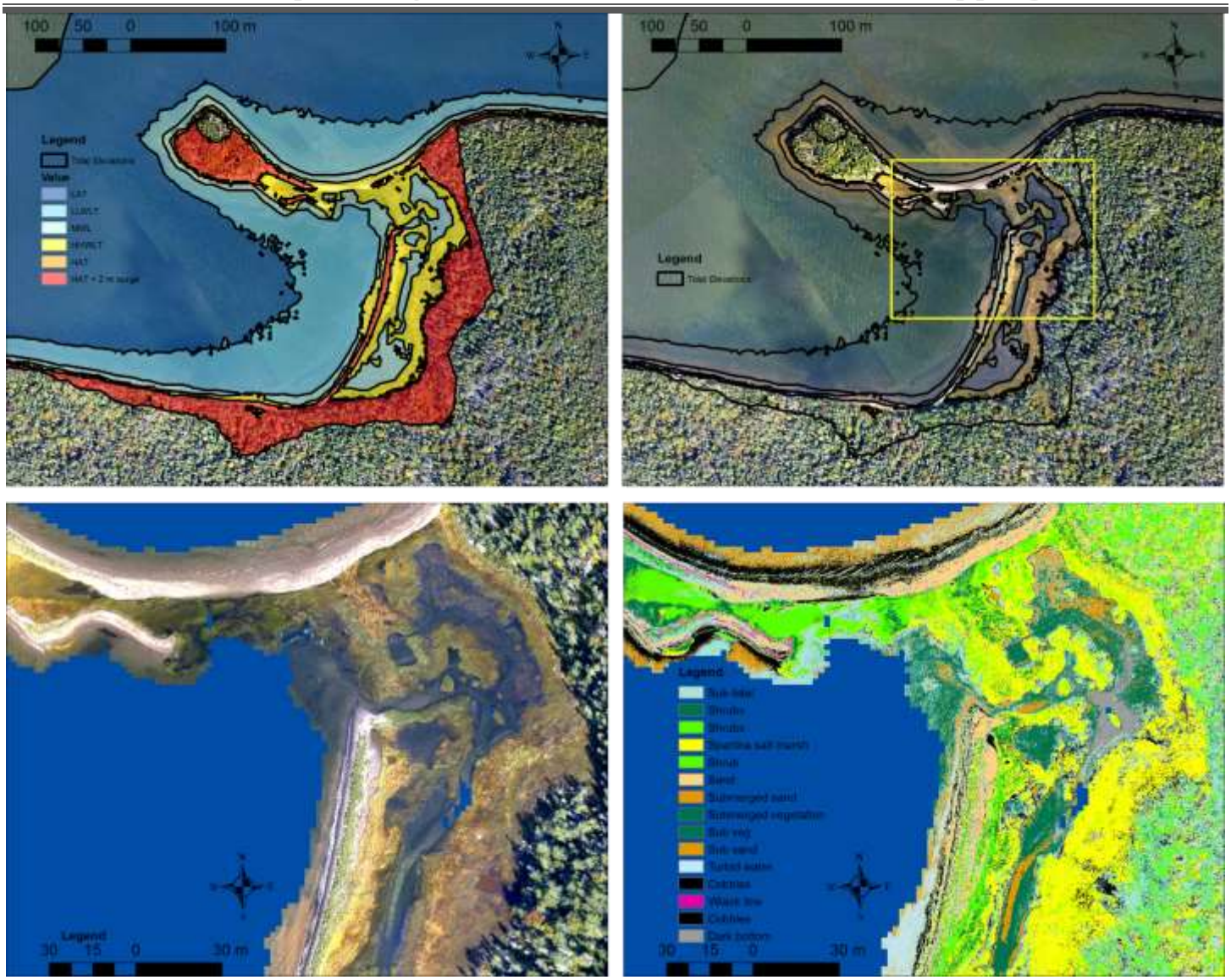

Figure 23 Study site 1, critical salt marsh habitat. Top left map is the tidal elevations from the lidar DEM. Top right map is the orthophoto mosaic with the vector outline of the tidal levels and with the detailed study area (yellow box). Bottom left is the RGB image with low lower water level superimposed. Bottom right is the classified salt marsh vegetation and sediment from the RCD30 imagery.

The RCD30 was also combined with the lidar DEM and derivatives such as slope to classify the shoreline components for study site 3 (Figure 24).

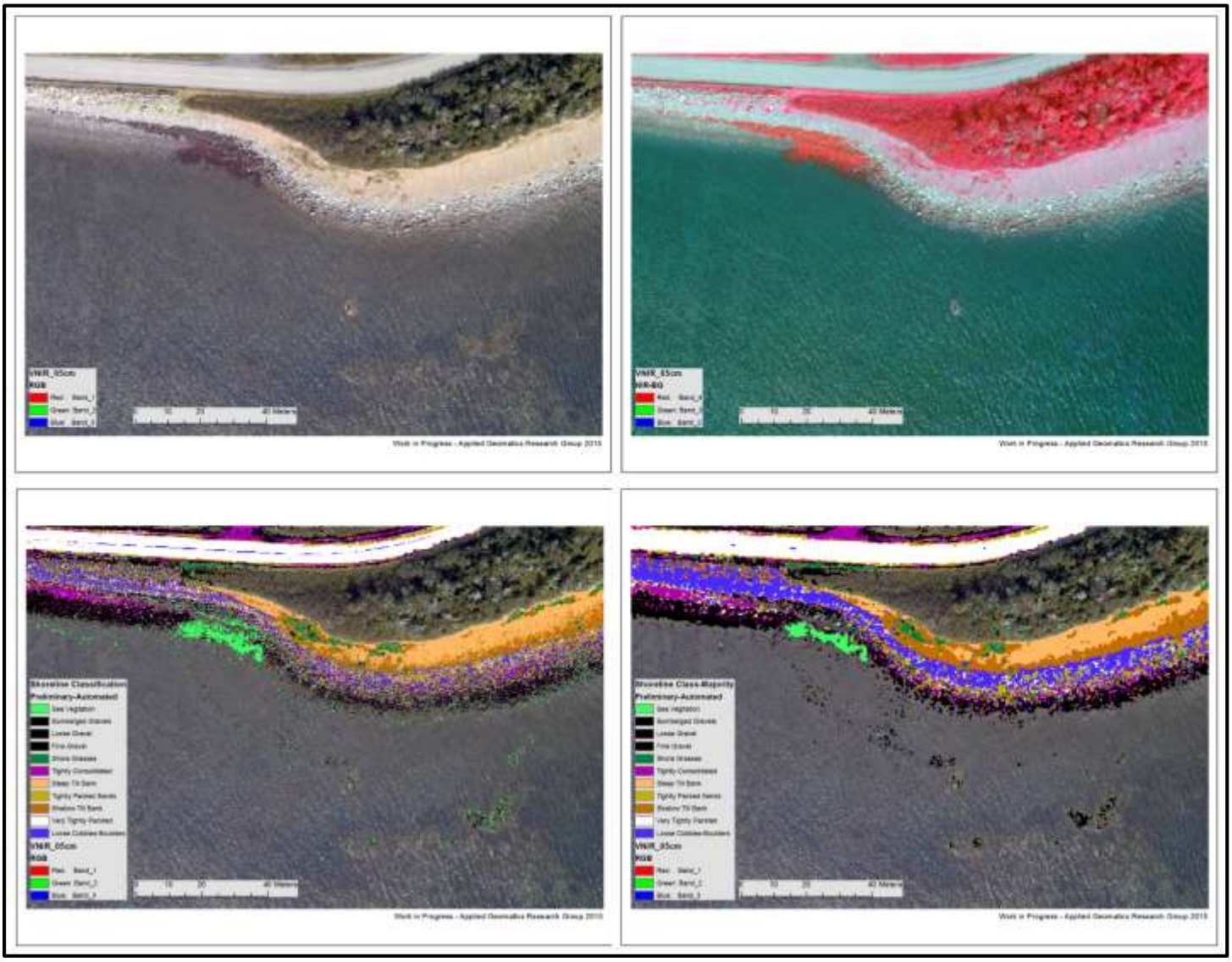

Figure 24 Example of RCD30+lidar classification results for study site 3. Top left is RGB RCD30 image. Top right is colour NIR image. Bottom left is the result of the classification. Bottom right is the classification with a majority filter applied.

4 Conclusions

The weather and water clarity conditions were not ideal for the survey and limited the depth of penetration. It is anticipated that the lidar would penetrate deeper in conditions when the water was clearer and not effected by wave and wind activity as is the case in late September. As a result lidar surveys should be planned when the wind conditions are at a minimum, which for this region is in mid-summer, July would be ideal.

The survey was successful in acquiring good data to a depth of approximately 6 m and thus highlights the most sensitive area of the intertidal and near sub tidal zone that could be effected if a contaminant spill were to occur. Several GIS

datasets were derived from the lidar an aerial photography as described in the report. The data will continue to be refined and processed to develop additional thematic map products that demonstrate how these data can support oil spill preparedness. More interaction with the end user community is required to better understand what type of enhanced products would be most useful to derive from these data. Over all this project has demonstrated the utility of the Chiroptera topo-bathymetric lidar sensor to acquire high quality data in the coastal zone to enhance decision making and better protect our coastal environment.

5 Appendix A Calibration Report

5.1 NSCC – Chiroptera Calibration Report

5.1.1 Calibration flight pattern

Calibration flight was done over the Fredericton downtown area. The calibration pattern consists of 4 lines, 3 parallel and one perpendicular. The middle and perpendicular lines are flown in both directions. The pattern is flown at two altitudes resulting in a total of 12 lines.

GPS base station was taken from the CanNet active network, well within 30 km of the calibration flight plan.

The calibration pattern was flown once at the start of the project and once at the end.

Calibration

Calibration is done in the automatic calibration tool which is part of Lidar Survey Studio.

Reference points were provided by Leading Edge Geomatics.

Results

Topo accuracy analysis

Accuracy analysis performed in Lidar Survey Studio using the following settings:

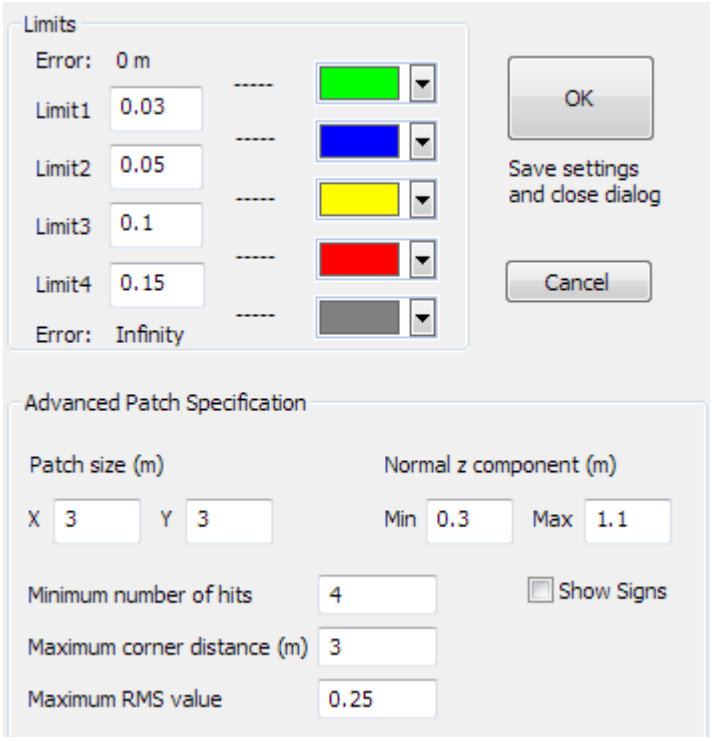

Topo - 400 m

Flightline accuracy between flightline 4 and flightline 2:

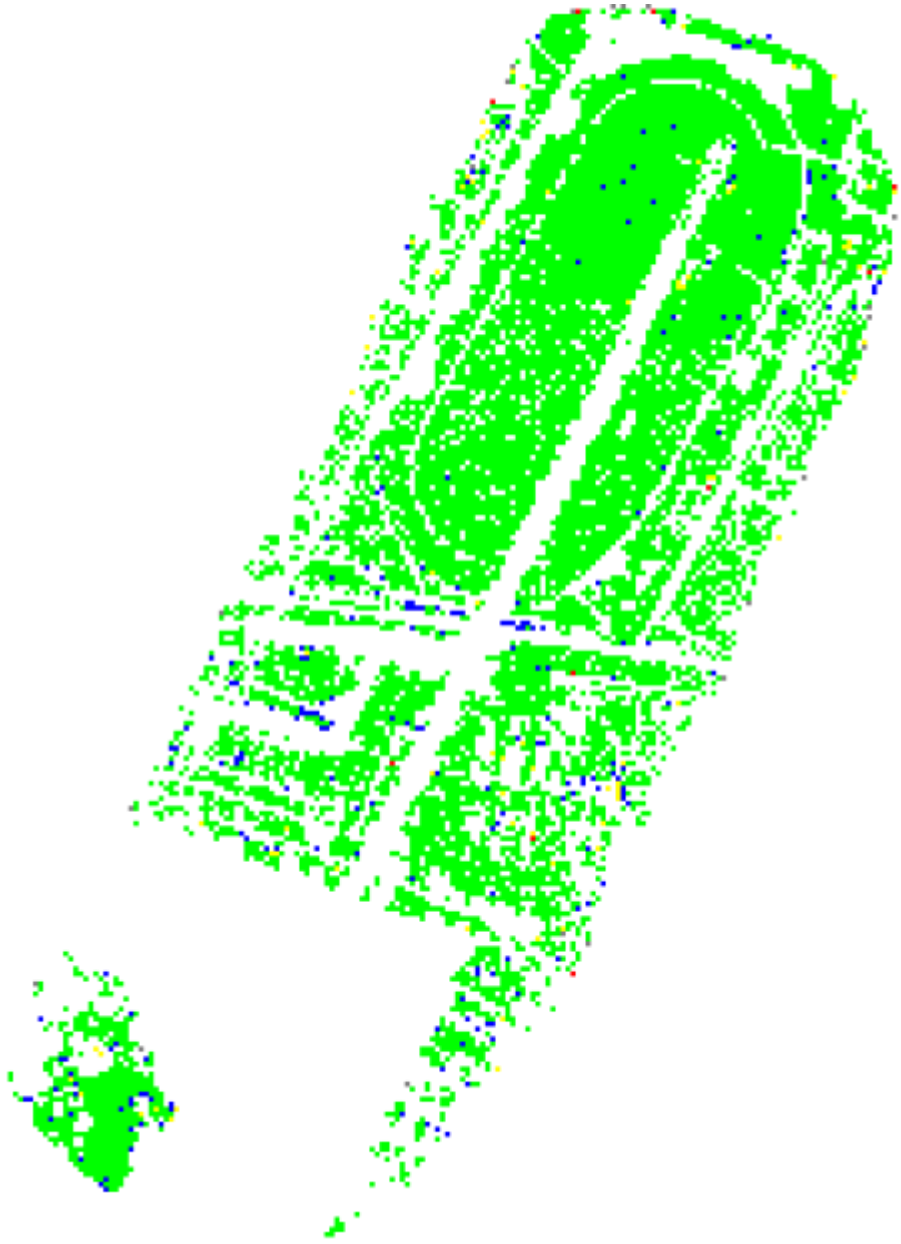

Flightline Accuracy Report Output:
ID003 Flightline 004 Topo 1 vs. ID008 Flightline 002 Topo 1 FL Accuracy

Limits	Patch#	First FL Positive	Average Error	Percentage
0.00 <= ERR <0.03	9748	48.16%	0.0063	96.63%
0.03 <= ERR <0.05	230	46.96%	0.0371	2.28%
0.05 <= ERR <0.10	78	56.41%	0.0657	0.77%
0.10 <= ERR <0.15	10	50.00%	0.1236	0.10%
0.15 <= ERR < Inf.	22	72.73%	0.4768	0.22%
Summary	10088	48.26%	0.0086	

Accuracy Index: 99

Patch Statistics
All#: 44707 | Valid: 26.60% | NumHit.fail:47.15% | ConDist.fail:0.37% | Normalz.fail:18.79% | RMS.fail:7.10%

Flightline accuracy between flightline 5 and flightline 7:

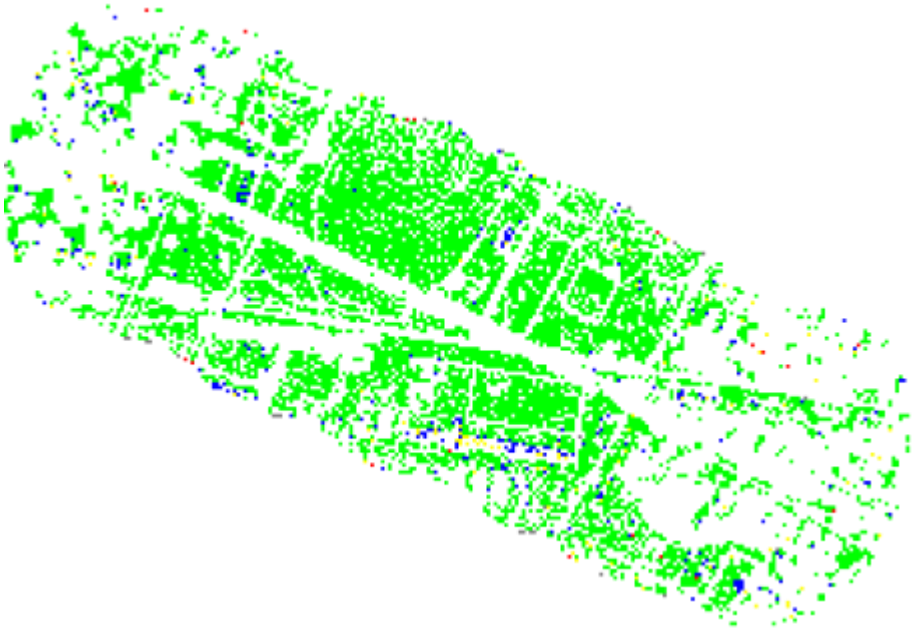

Flightline Accuracy Report Output:
ID005 Flightline 005 Topo 1 vs. ID007 Flightline 006 Topo 1 FL Accuracy

Limits	Patch#	First FL Positive	Average Error	Percentage
0.00 <= ERR <0.03	8505	20.53%	0.0086	94.76%
0.03 <= ERR <0.05	302	18.87%	0.0370	3.36%
0.05 <= ERR <0.10	121	13.22%	0.0640	1.35%
0.10 <= ERR <0.15	21	38.10%	0.1237	0.23%
0.15 <= ERR < Inf.	26	38.46%	0.6219	0.29%
Summery	8975	20.47%	0.0124	

Accuracy Index: 98

Patch Statistics
All#: 46182 | Valid: 23.14% | Nummit.fail:44.79% | Conplst.fail:0.26% | Normalz.fail:19.51% | RMS.fail:12.30%

Scan accuracy flightline 4:

Scan Accuracy Report Output:
ID003 Flightline 004 Topo 1+ID003 Flightline 004 Topo 1 Scan Accuracy

Limits	Patch#	Front Scan Positive	Average Error	Percentage
0.00 <= ERR <0.03	10191	65.59%	0.0057	96.85%
0.03 <= ERR <0.05	202	53.47%	0.0381	1.92%
0.05 <= ERR <0.10	79	49.37%	0.0633	0.75%
0.10 <= ERR <0.15	20	65.00%	0.1166	0.19%
0.15 <= ERR < Inf.	31	54.84%	0.3671	0.29%
Summery	10523	65.20%	0.0081	

Accuracy Index: 98

Patch Statistics
All#: 56842 | Valid: 21.69% | NumHit.fail:55.93% | ConDist.fail:0.29% | Normalz.fail:15.57% | RMS.fail:6.52%

Hydro accuracy analysis

Accuracy analysis performed in Lidar Survey Studio using the following settings:

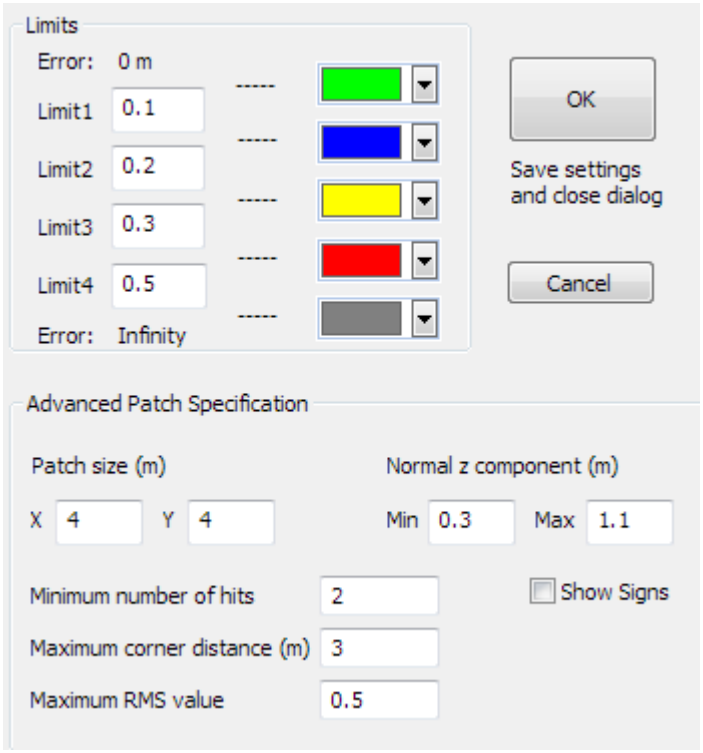

Flightline accuracy between flightline 4 and flightline 2:

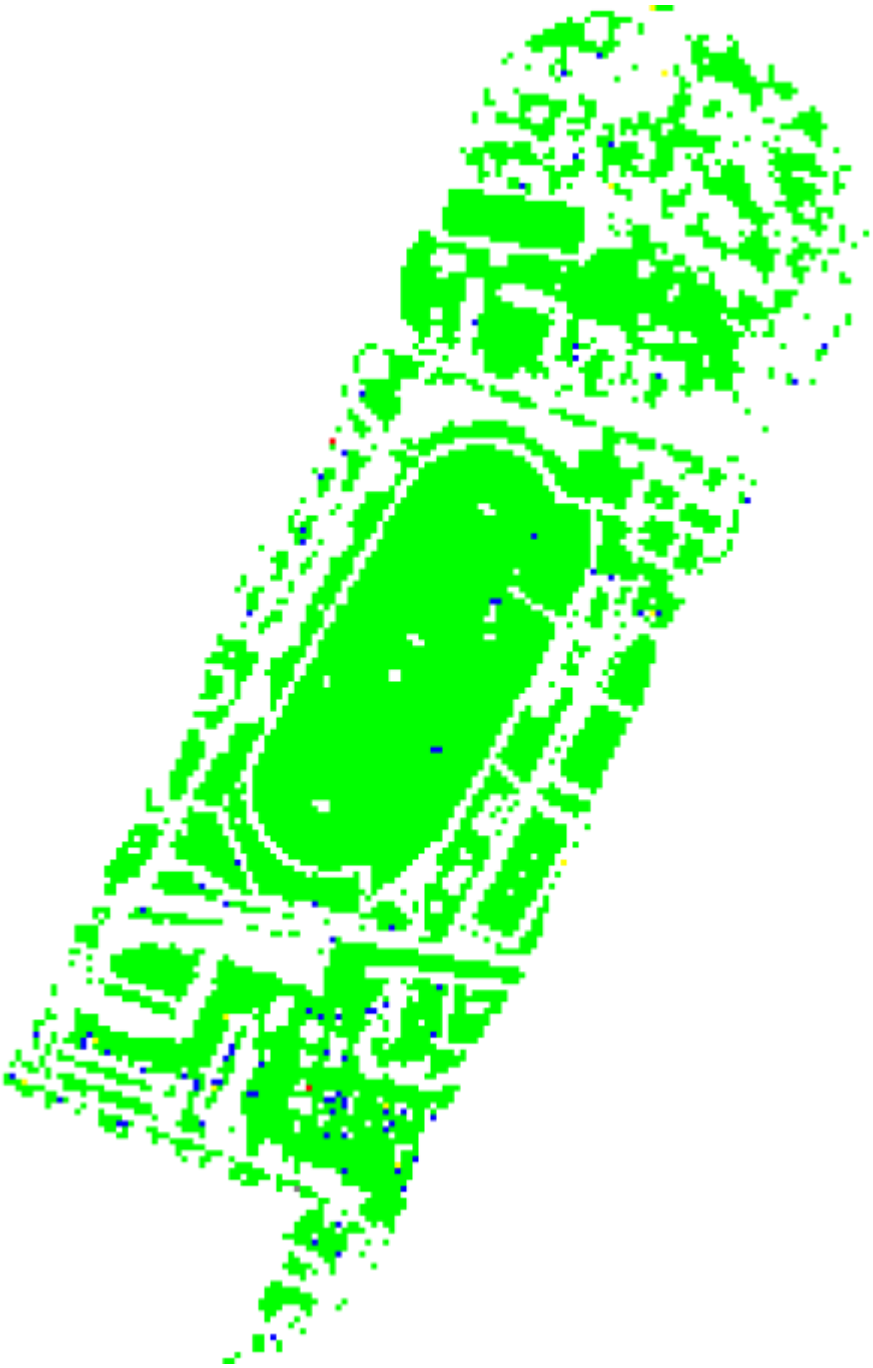

Flightline Accuracy Report Output:
ID003 Flightline 004 Shallow vs. ID008 Flightline 002 Shallow FL Accuracy

Limits	Patch#	First FL Positive	Average Error	Percentage
0.00 <= ERR <0.10	7913	54.93%	0.0126	98.74%
0.10 <= ERR <0.20	87	49.43%	0.1343	1.09%
0.20 <= ERR <0.30	11	81.82%	0.2471	0.14%
0.30 <= ERR <0.50	2	50.00%	0.3120	0.02%
0.50 <= ERR < Inf.	1	100.00%	0.5226	0.01%
Summery	8014	54.92%	0.0144	

Accuracy Index: 99

Patch Statistics
All#: 35037 | Valid: 25.15% | NumHit.fail:50.59% | Condist.fail:0.83% | Normalz.fail:18.47% | RMS.fail:4.95%

Scan accuracy, flightline 2:

Scan Accuracy Report Output:
ID008 Flightline 002 shallow Scan Accuracy

Limits	Patch#	Front Scan Positive	Average Error	Percentage
0.00 <= ERR <0.10	7140	20.49%	0.0166	97.98%
0.10 <= ERR <0.20	116	31.90%	0.1342	1.59%
0.20 <= ERR <0.30	21	28.57%	0.2337	0.29%
0.30 <= ERR <0.50	8	0.00%	0.3589	0.11%
0.50 <= ERR < Inf.	2	100.00%	1.3212	0.03%
Summery	7287	20.69%	0.0198	

Accuracy Index: 99

Patch Statistics
All#: 42237 | Valid: 19.00% | NumHit.fail:62.76% | ConDist.fail:0.79% | Normalz.fail:14.28% | RMS.fail:3.17%

Comparison between first and second calibration flight

Topo, flightline accuracy

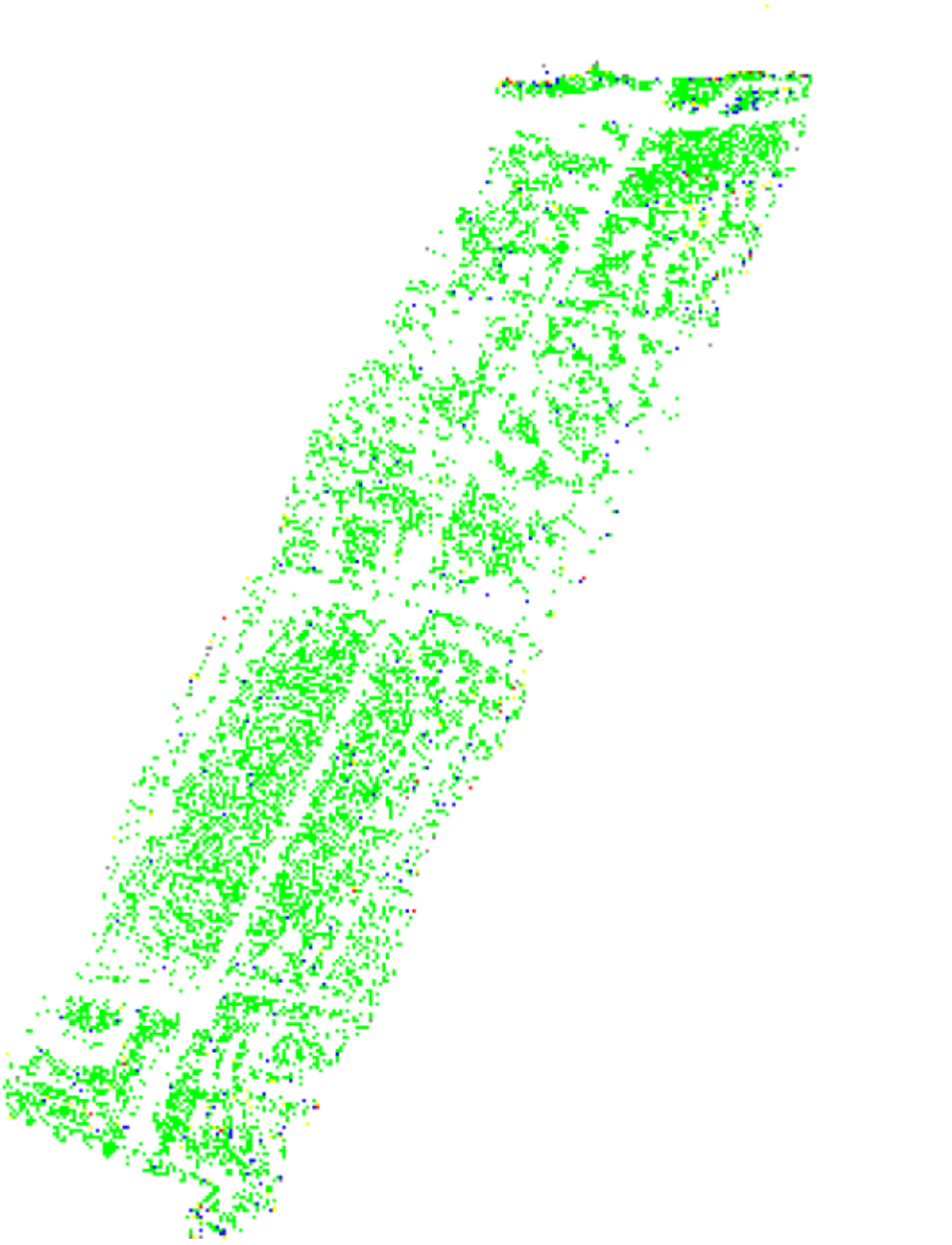

Flightline Accuracy Report Output:
ID003 Flightline 004 Topo 1 vs. ID005 Flightline 004 Topo 1 FL Accuracy

Limits	Patch#	First FL Positive	Average Error	Percentage
0.00 <= ERR <0.03	7921	32.37%	0.0073	95.16%
0.03 <= ERR <0.05	210	50.95%	0.0378	2.52%
0.05 <= ERR <0.10	122	48.36%	0.0673	1.47%
0.10 <= ERR <0.15	25	52.00%	0.1216	0.30%
0.15 <= ERR < Inf.	46	50.00%	0.3543	0.55%
Summery	8324	33.23%	0.0112	

Accuracy Index: 98

Patch Statistics
All#: 90768 | Valid: 15.18% | NumHit.fail:59.84% | Condist.fail:0.27% | Normalz.fail:11.01% | RMS.fail:13.70%

Hydro, flightline accuracy

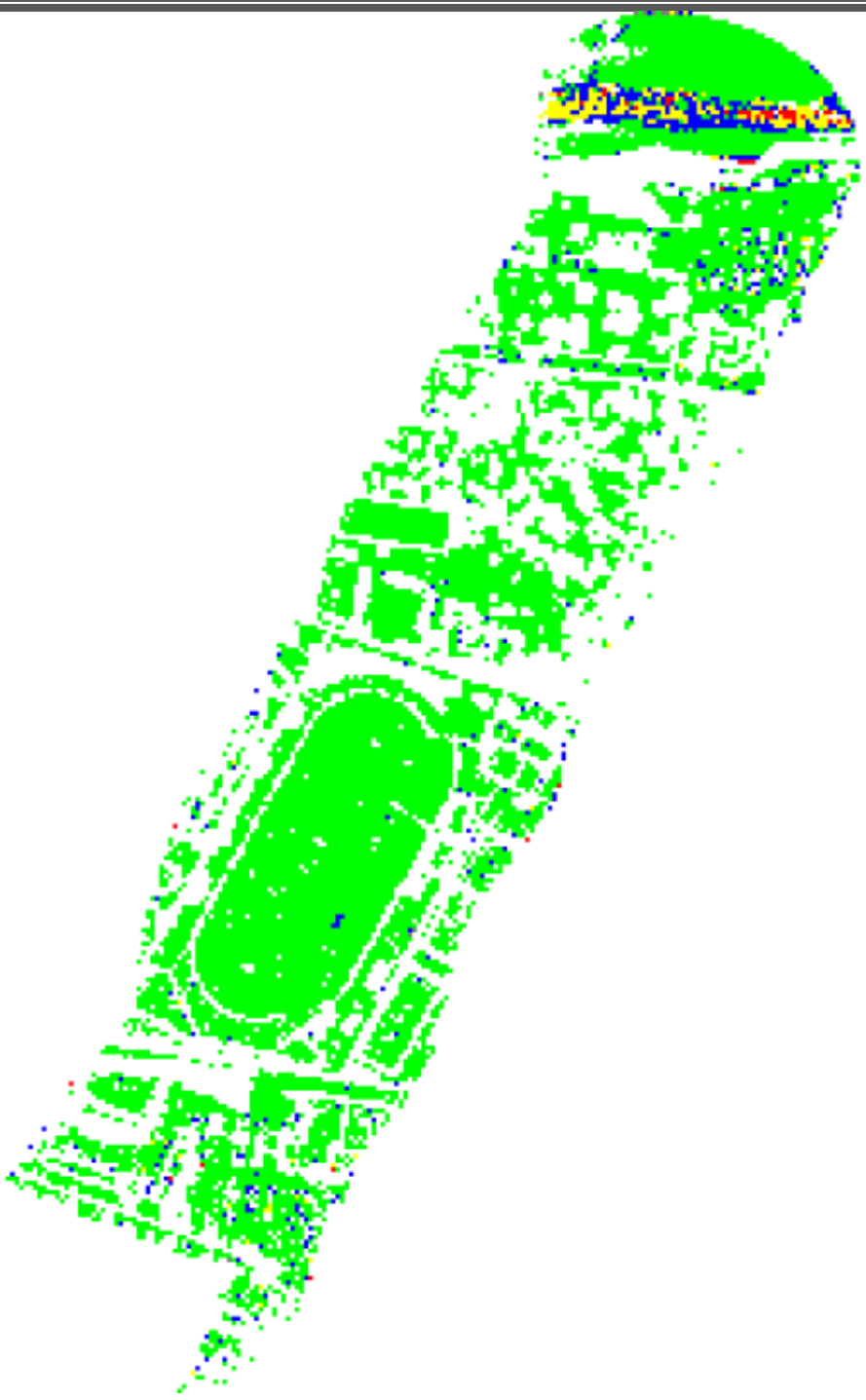

Flightline Accuracy Report Output:
ID003 Flightline 004 shallow vs. ID005 Flightline 004 shallow FL Accuracy

Limits	Patch#	First FL Positive	Average Error	Percentage
0.00 <= ERR <0.10	10195	74.44%	0.0208	92.65%
0.10 <= ERR <0.20	514	85.99%	0.1415	4.67%
0.20 <= ERR <0.30	232	95.69%	0.2395	2.11%
0.30 <= ERR <0.50	49	93.88%	0.3457	0.45%
0.50 <= ERR < Inf.	14	50.00%	0.7939	0.13%
Summery	11004	75.48%	0.0335	

Accuracy Index: 97

Patch Statistics
All#: 59976 | Valid: 25.18% | Nummit.fail:59.96% | Condist.fail:0.77% | Normalz.fail:8.72% | RMS.fail:5.36%

Comparison with reference points

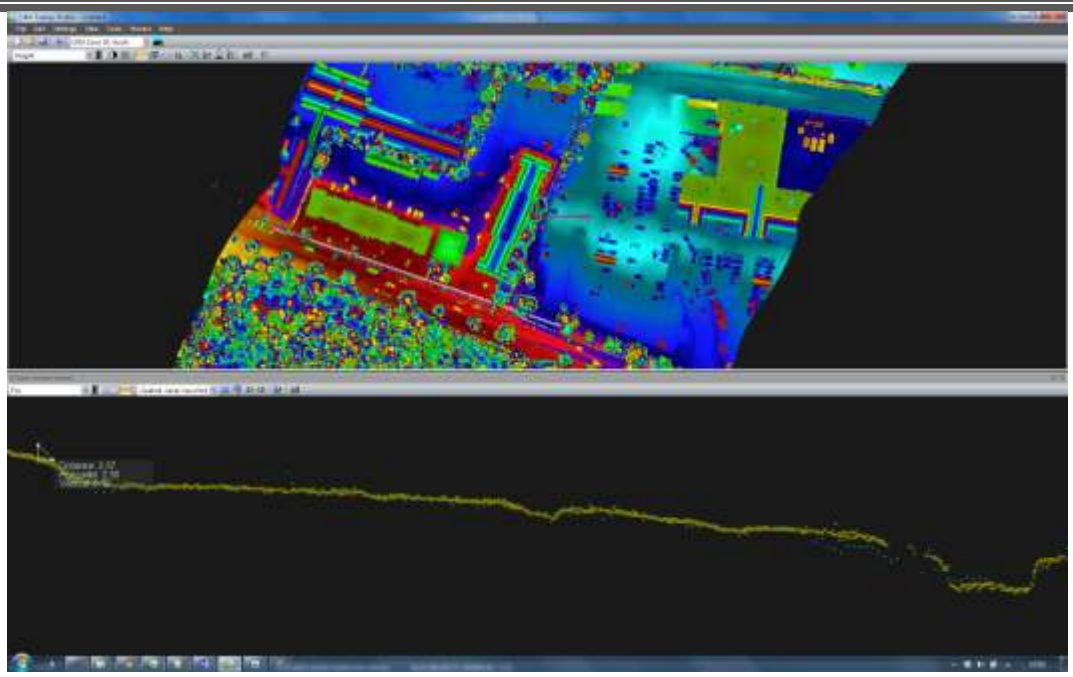

The image above shows one line from each laser, green is from the bathymetric laser, yellow from the topographic. Red are RTK reference points. Ruler inserted for scale.

6 Appendix B Data Dictionary

Atlantic Canadian Bathymetric Lidar Collection

Documentation to Accompany Data Delivery

Provided by:

Tim Webster, PhD
Kevin McGuigan, Nathan Crowell
Applied Geomatics Research Group
NSCC, Middleton
Tel. 902 825 5475
email: tim.webster@nscc.ca

In submission to:

Pêches et Océans Canada | Fisheries and Oceans Canada

Fisheries and Oceans Canada

Overview

A total of **72.6 GB** of raw and derivative data collected from the pilot bathymetric lidar campaign has been provided along with this document for submission in accordance with the DFO initiative for developing lidar-based seabed habitat mapping. Data included in the submission is in accordance with the deliverables as proposed

- 201503_ILSE_MADAME
  - Colour_Shaded_Relief
  - Control
  - Grids
  - LAS
  - Orthomosaics
  - Report
  - Shoreline_Classification

Data provided was collected September 27, 2014 using a Leica-AHAB Chiroptera II Topo-Bathymetric airborne lidar system. The system incorporates a Leica RCD30 camera system for high resolution visible-near infrared photography.

Study areas collected include the South West coast of Ilse Madame Island (Cape Breton, Nova Scotia). The entirety of the survey was conducted at

Colour Shaded Relief

Several variants of the color shade relief (CSR) graphical display method have been delivered including those with, and with-out the inclusion of lidar reflectance values. All CSR products contain a combination of colorized lidar elevation data and a hill shade relief model. CSR products are delivered for both lidar elevation products: Digital Elevation Models (DEMs) which contain only ground and bathymetric points, as well as Digital Surface Models (DSM) which contain all valid lidar returns (trees, power lines, etc…)

Control

Control data such as aircraft trajectory information, time of flight GPS base station information, and hard surface differential GPS validation measurements have been included as outlined in the accompanying report.

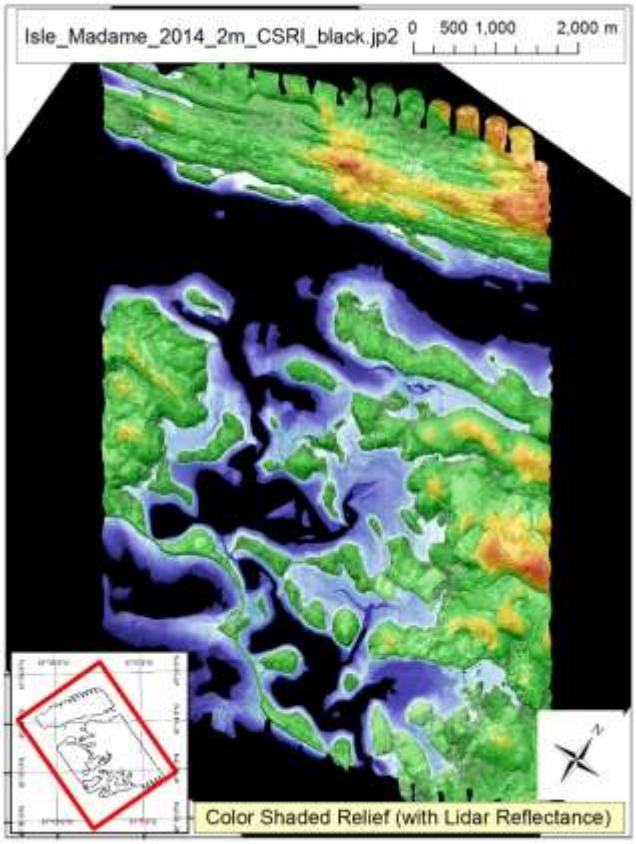

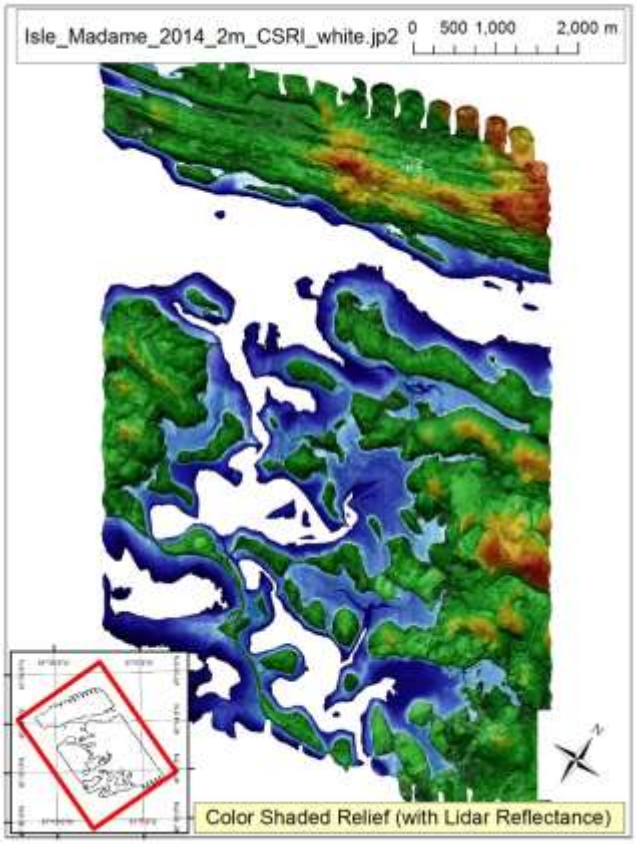

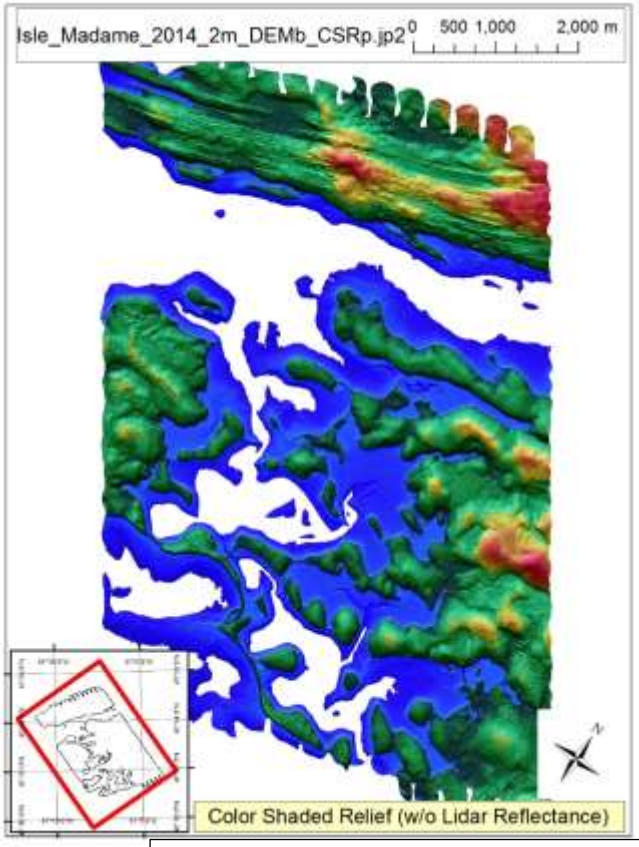

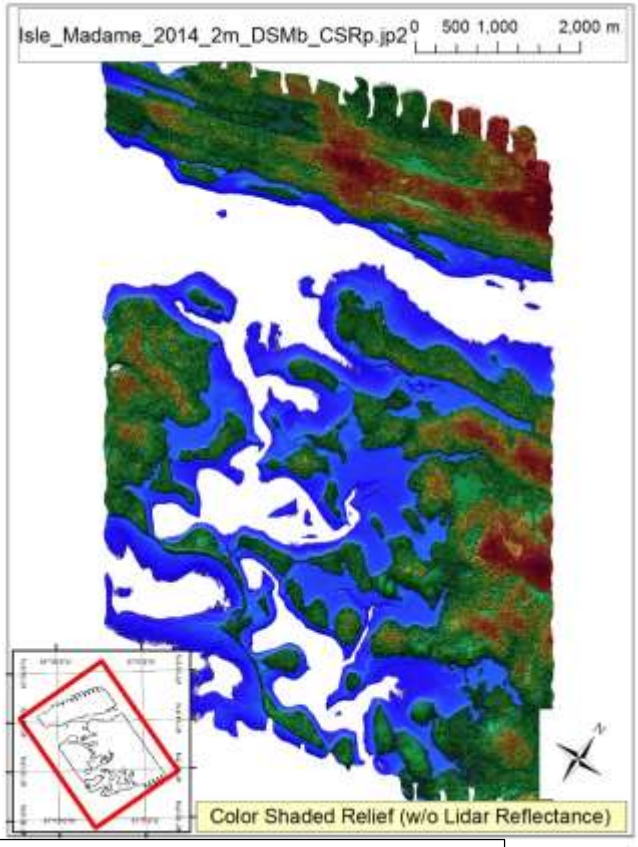

201503 ILSE MADAME > Colour Shaded relief

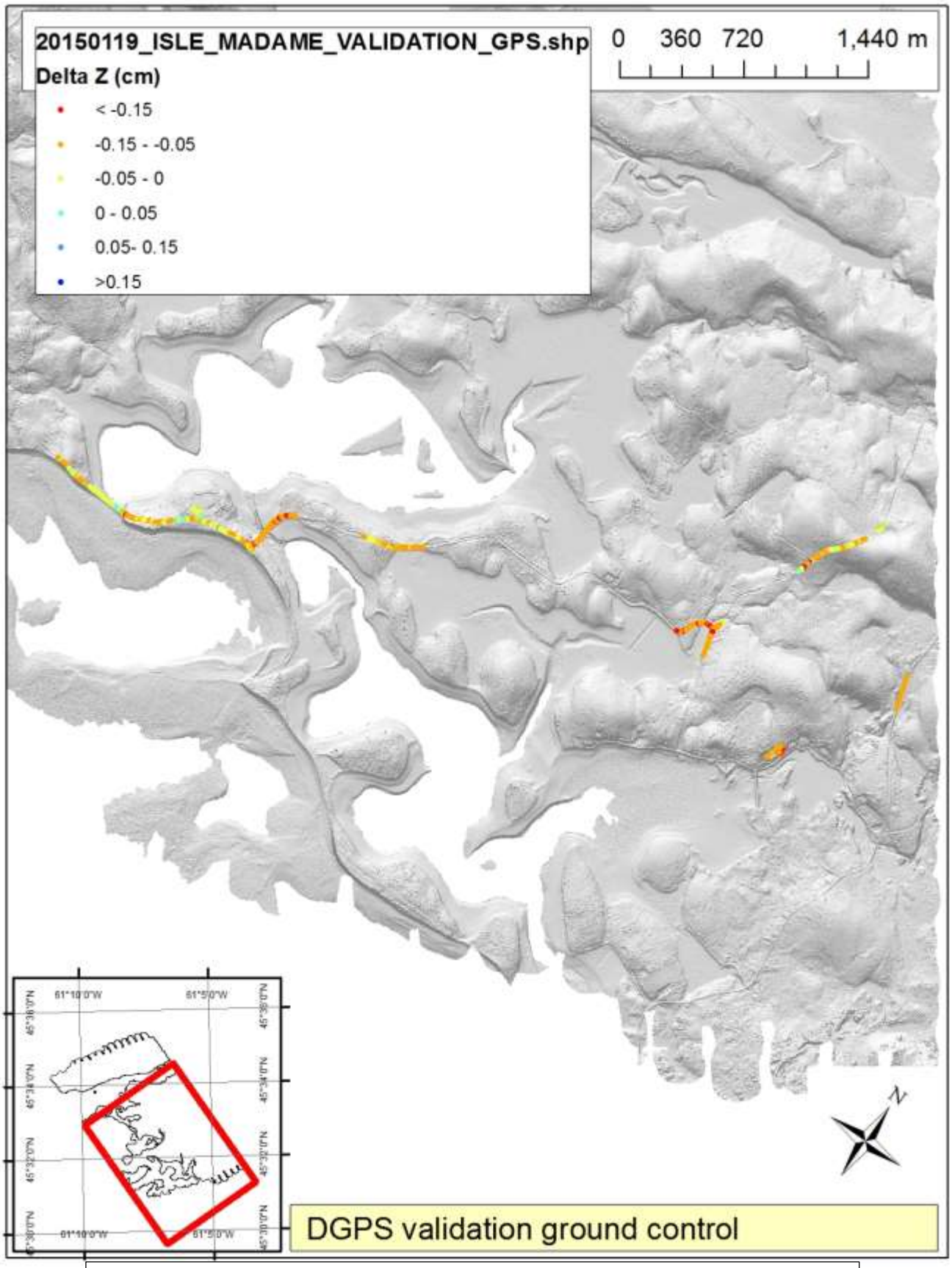

201503 ILSE MADAME > Control

Grids

Topographic bathymetric grid data is presented as two variants; *Digital Surface Models* (DSM), and *Digital Elevation models (*DEM). Both data variants are constructed using bathymetric sea bed laser returns; combined with infrared topo-laser returns over land features. Land features include all ground (fields, forest bottom, roads etc.) as well as valid non-ground land features (trees, vegetation, buildings, power lines, etc…). DEMs are built from bathymetric and all ground returns only (ie, no trees, power lines etc… included) whereas DSMs additionally include all valid non-ground laser returns.

All lidar derived grid datasets are delivered in a geographic .TIF raster format; each with a spatial resolution of 2 meters as 32-bit depth floating point, and suitable to be viewed in ArcGIS. Grid data is stored in the *Universal Transverse Mercator* projection (UTM, Zone 20N) and referenced to the *North American Datum 1983* (NAD83). Grid data which contains elevation data (DEMs, DSMs, and water surface models) are referenced to the Canadian Geodetic Vertical datum (CGVD28, HT2) whereas lidar reflectance grids contain relative values representative of lidar pulse return intensity. The lidar reflectance information delivered is derived from the green bathymetric channel laser of the Chiroptera II for seabed and on ground laser pulse returns.

Las

3-d point cloud of all lidar returns (ie. Ground features, vegetation, sea surface, and seabed). This data is presented in the form of classified .LAS files. Point data is stored in the *Universal Transverse Mercator* projection (UTM, Zone 20N) and referenced to the *North American Datum 1983* (NAD83) including the *Geodetic Reference System 1980* (GRS80). Elevation information for the point datasets is referenced to the ellipsoid.

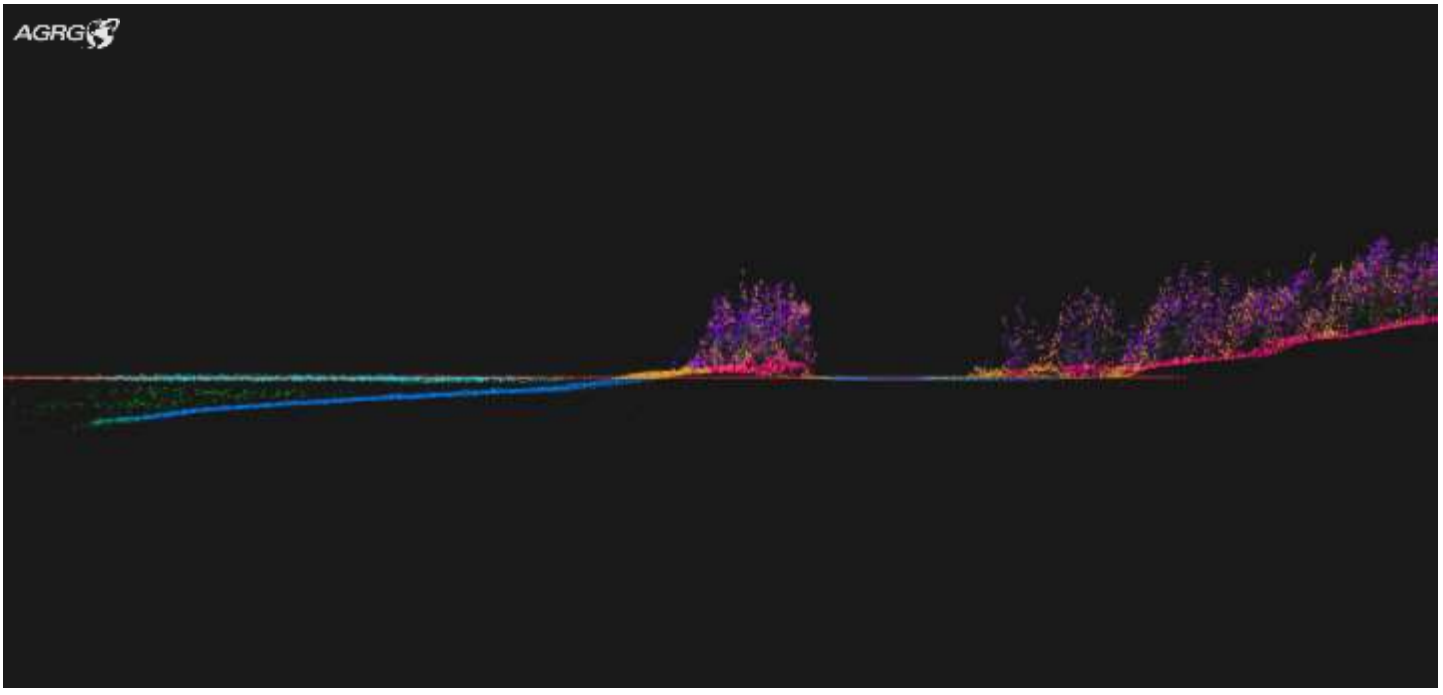

**An example of the dense topo-bathymetric lidar point cloud illustrated in cross-section; captured around the northern portion of the Ilse Madame Study Area. (Blue: shallow water bathymetric points; Purple/Pink: Canopy and Forest floor point data.)*

This data is provided in 500m square blocks, each containing all overlapping flight lines and classified as follows:

Classification Code	Lidar Point Classification Description
0	Modelled water surface
1	Bathymetric seabed
2	Underwater Vegetation
3	N/A
4	NIR Topo-laser Ground
5	NIR Topo-laser Non-Ground
6	Green bathymetric-laser Ground
7	Green bathymetric-laser Non-Ground
8	Measured water surface
9	Noise
10	*Overlapping Modelled water surface*
11	*Overlapping Bathymetric seabed*
12	*Overlapping Underwater Non-Ground*
13	*N/A*
14	*Overlapping NIR Topo-laser Ground*
15	*Overlapping NIR Topo-laser Non-Ground*
16	*Overlapping Green bathymetric-laser Ground*
17	*Overlapping Green bathymetric-laser Non-Ground*
18	*Overlapping Measured water surface*
19	*Overlapping Noise*

*note that 'overlap' is determined for points which are within a desired footprint of points from a separate flight line; the latter of which having less absolute range to the laser sensor.

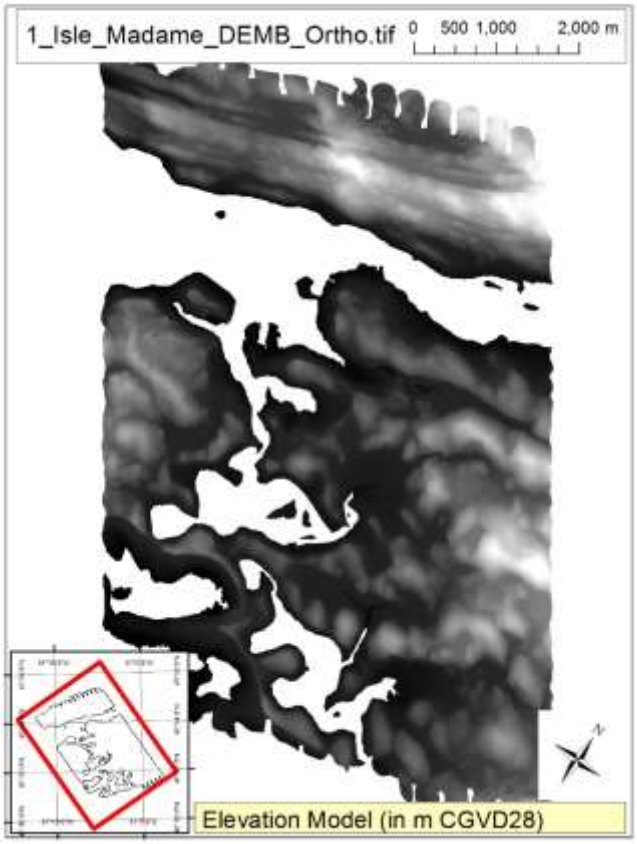

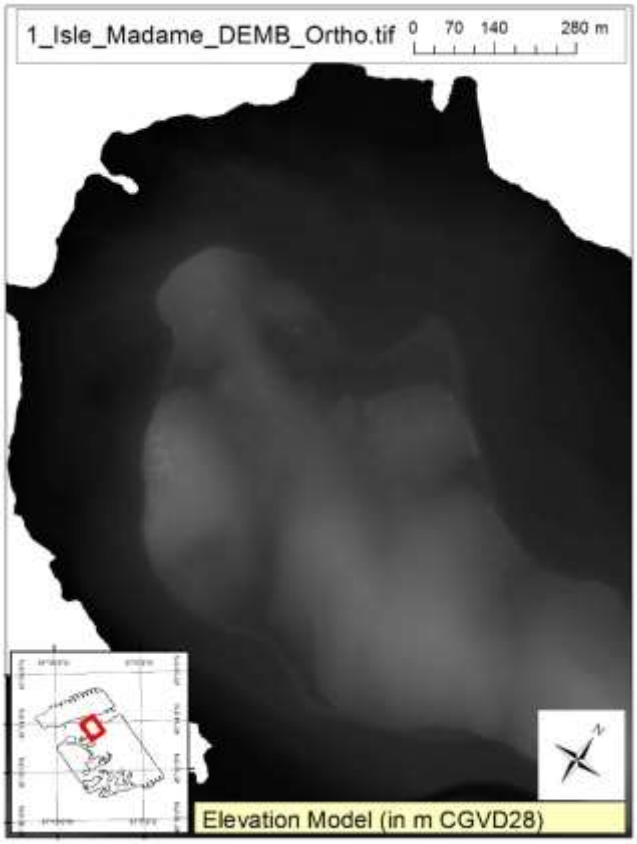

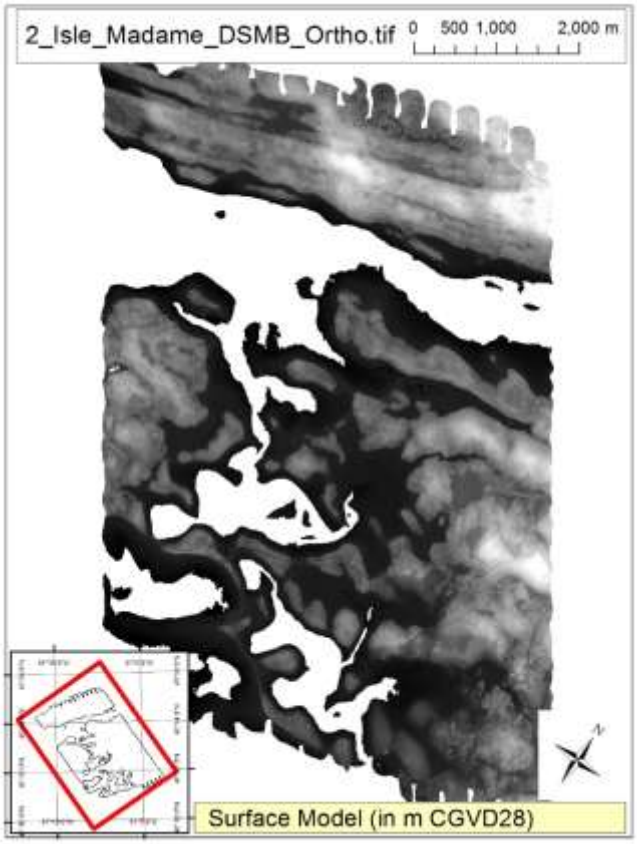

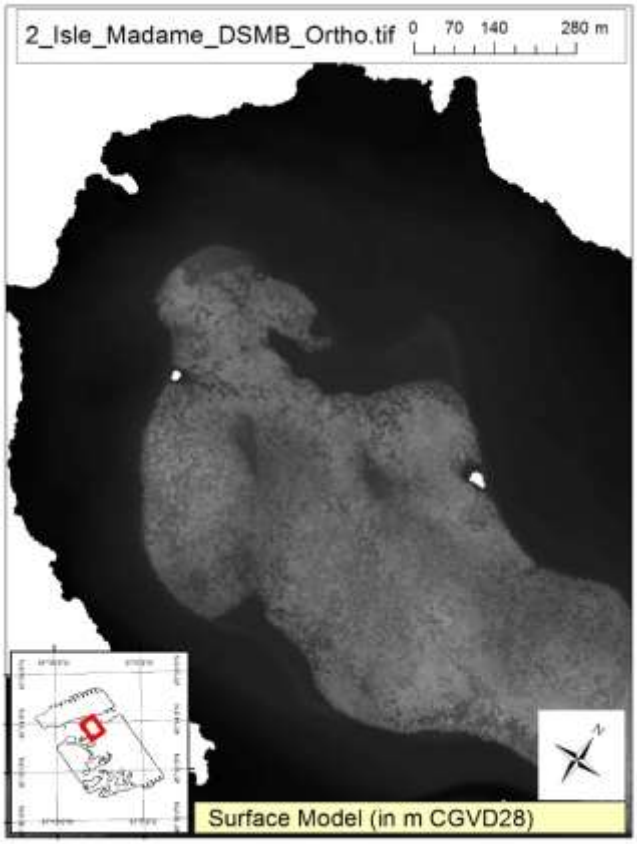

201503 ILSE MADAME > Grids

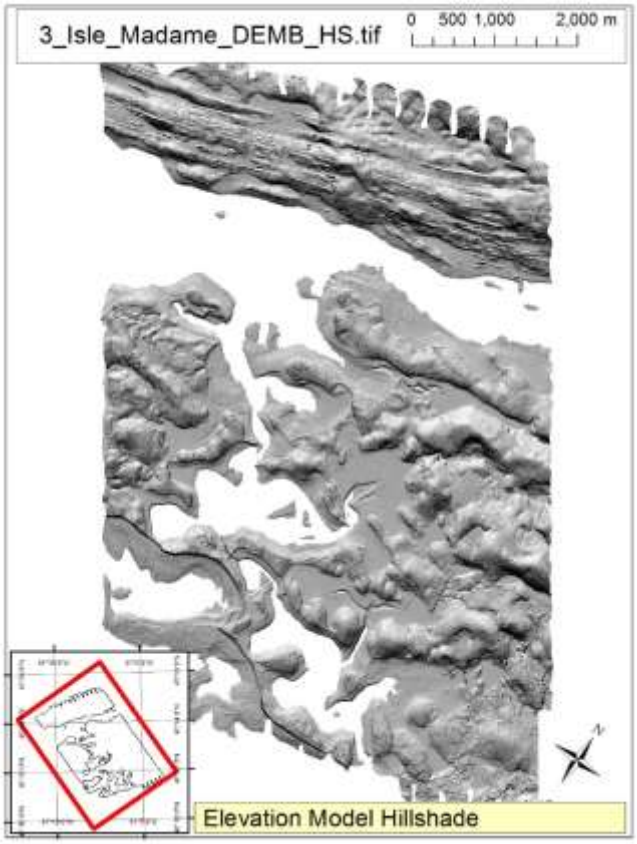

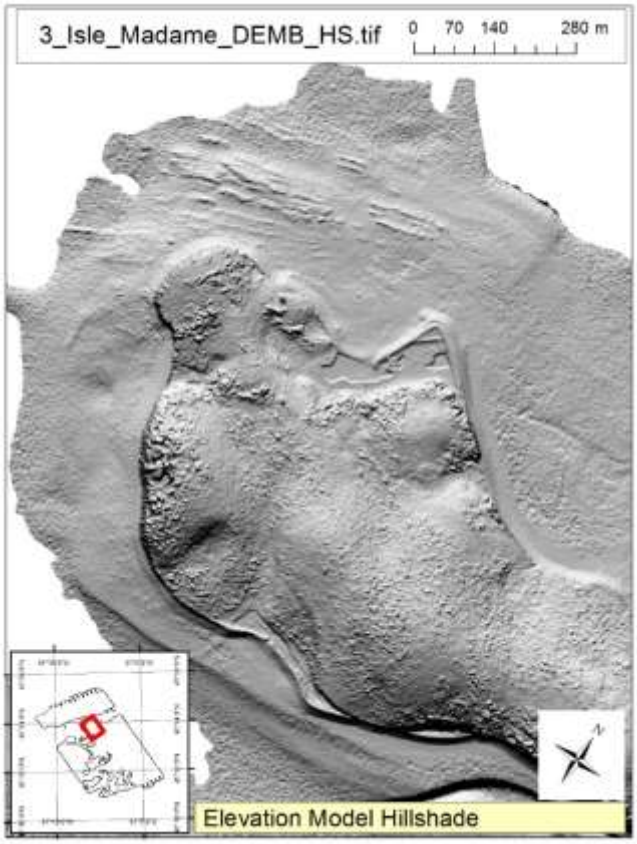

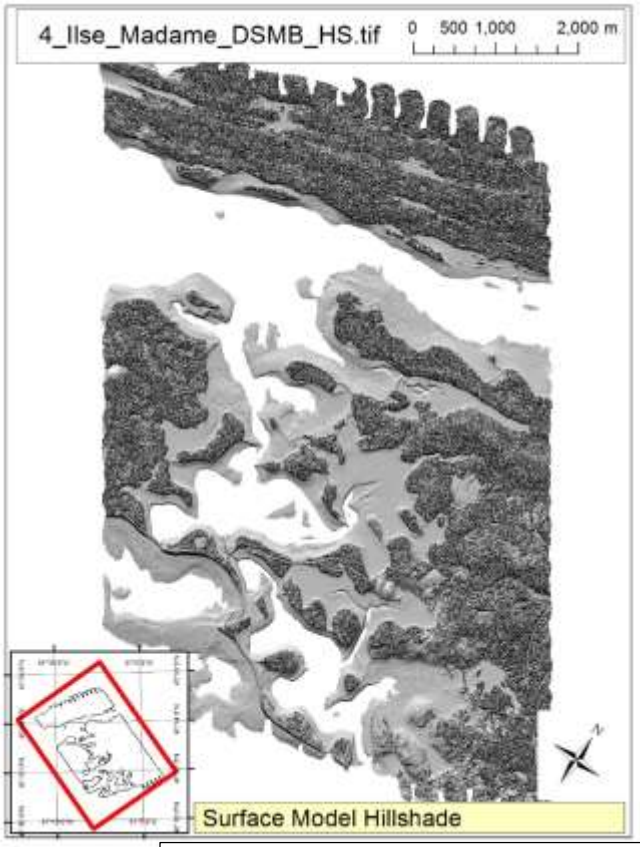

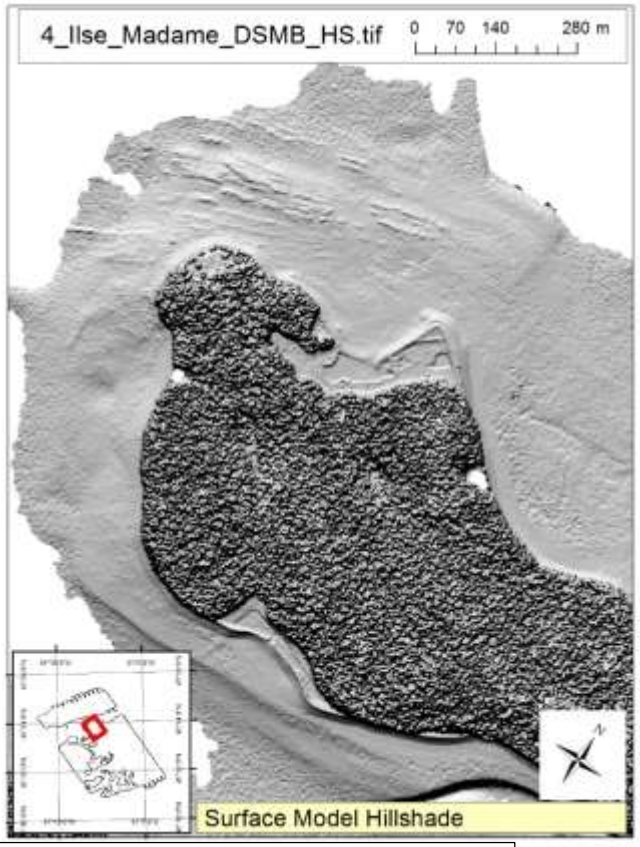

201503 ILSE MADAME > Grids

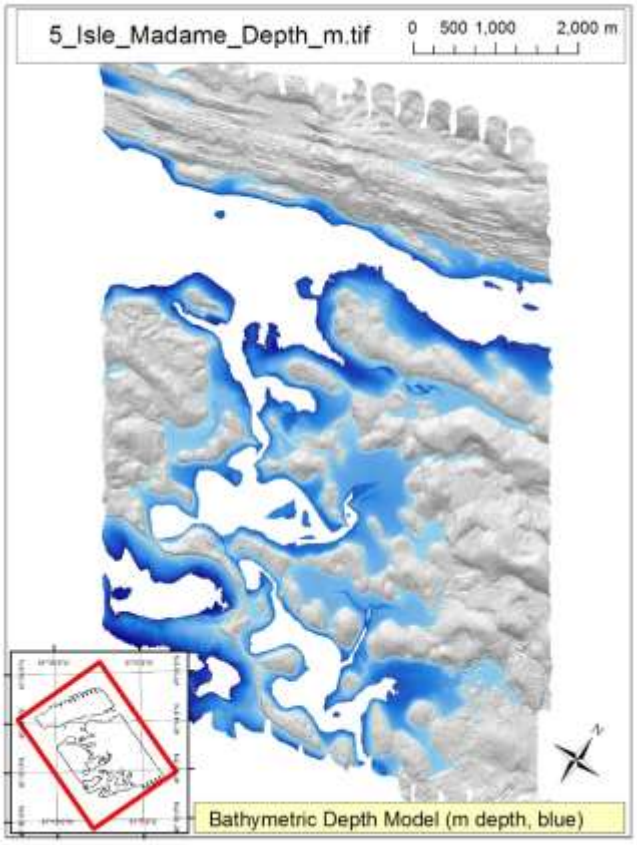

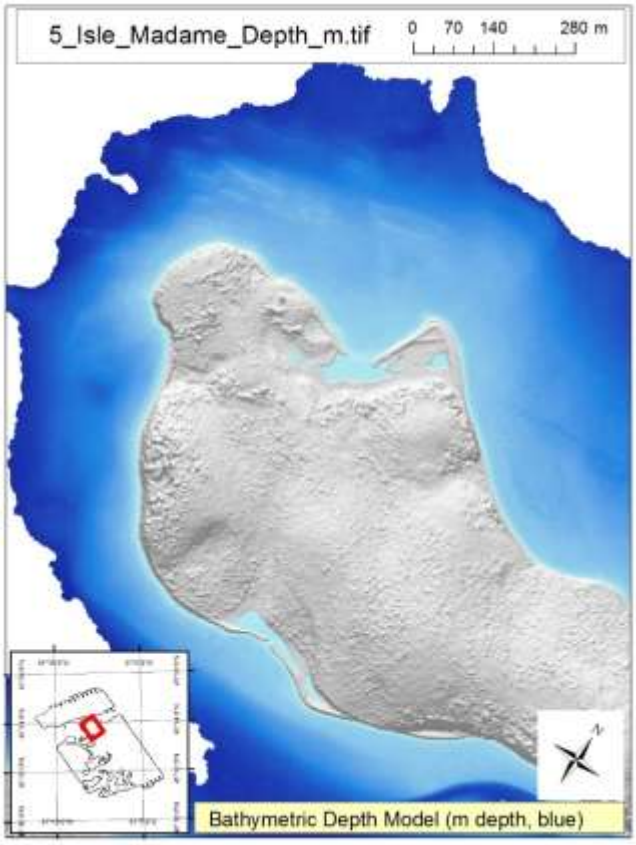

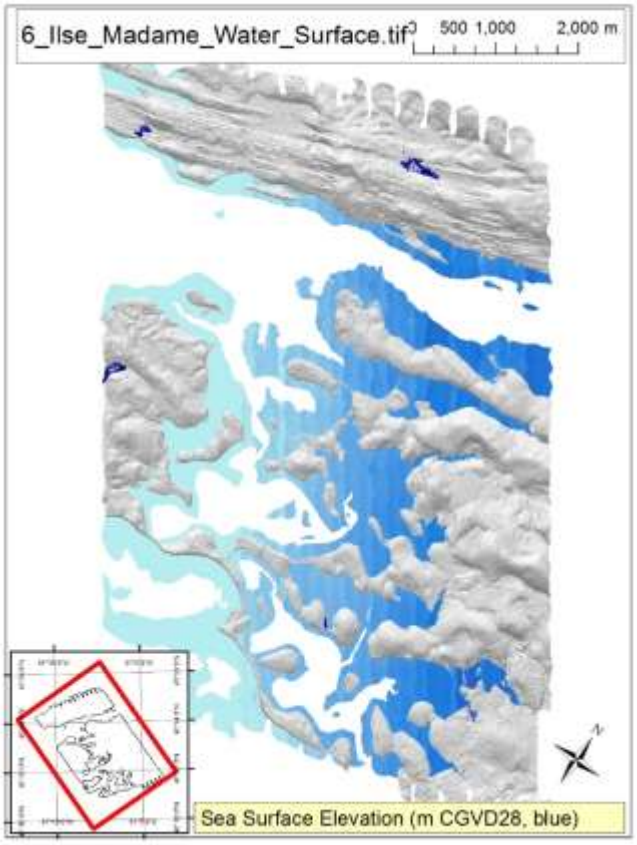

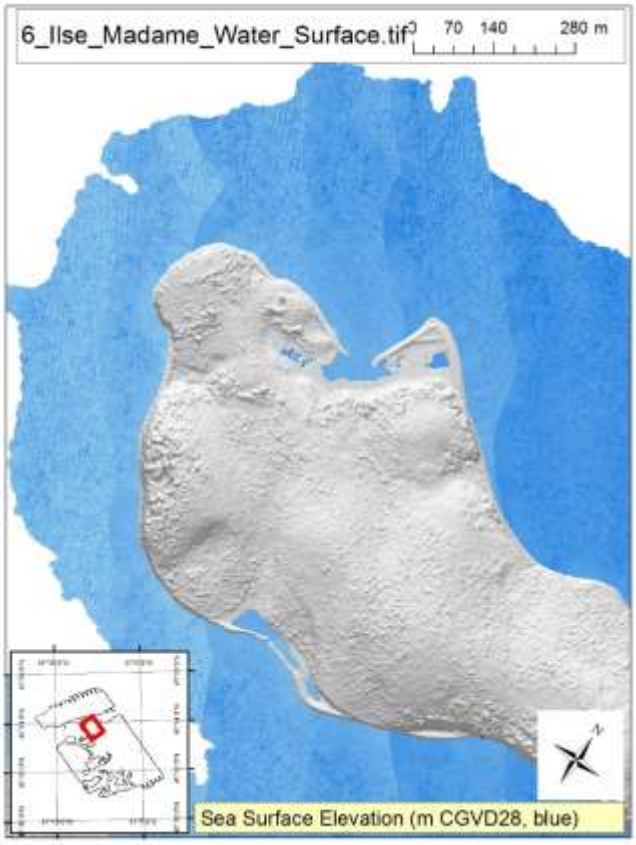

201503 ILSE MADAME > Grids

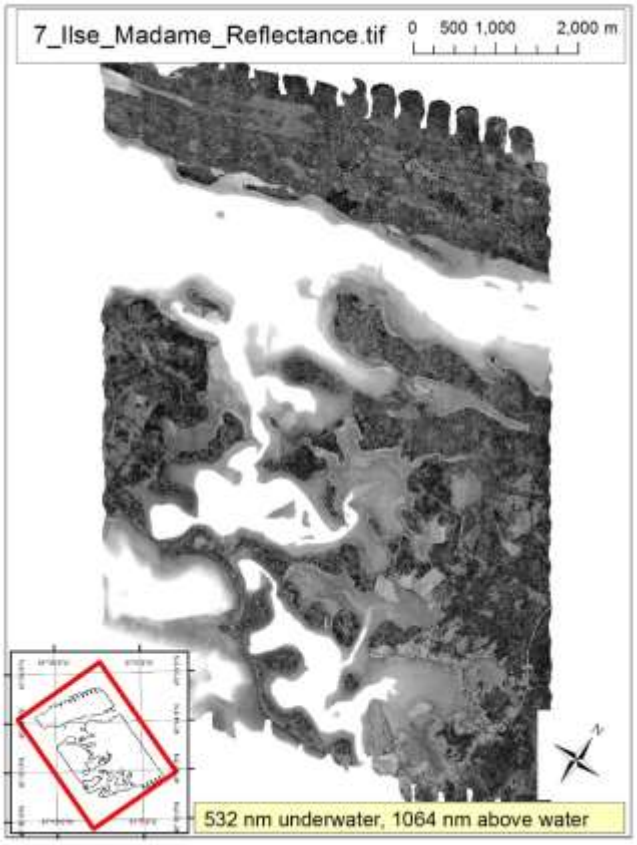

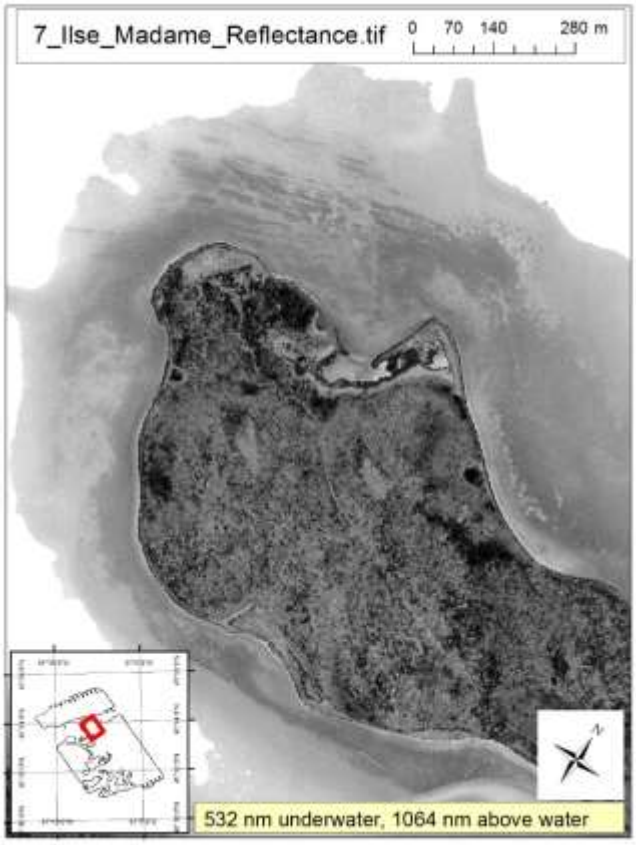

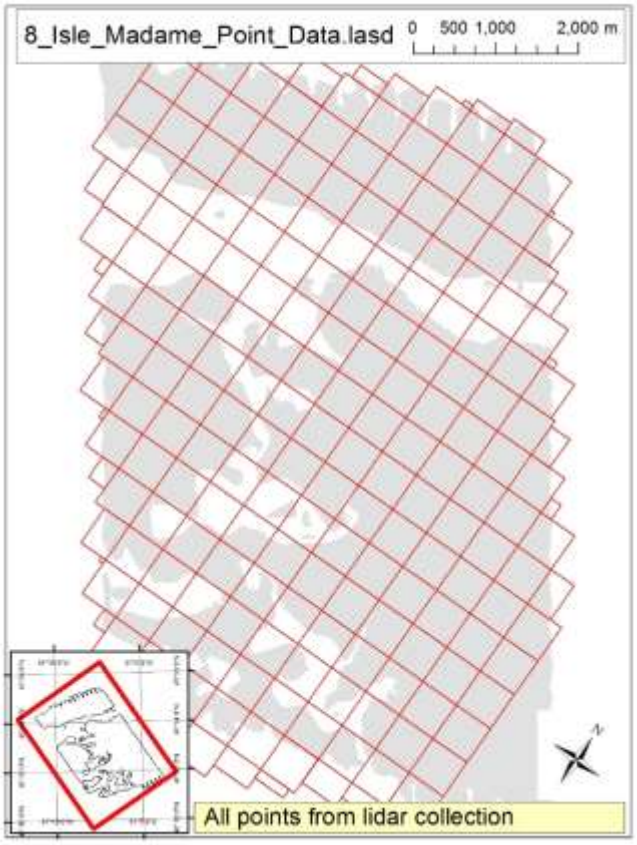

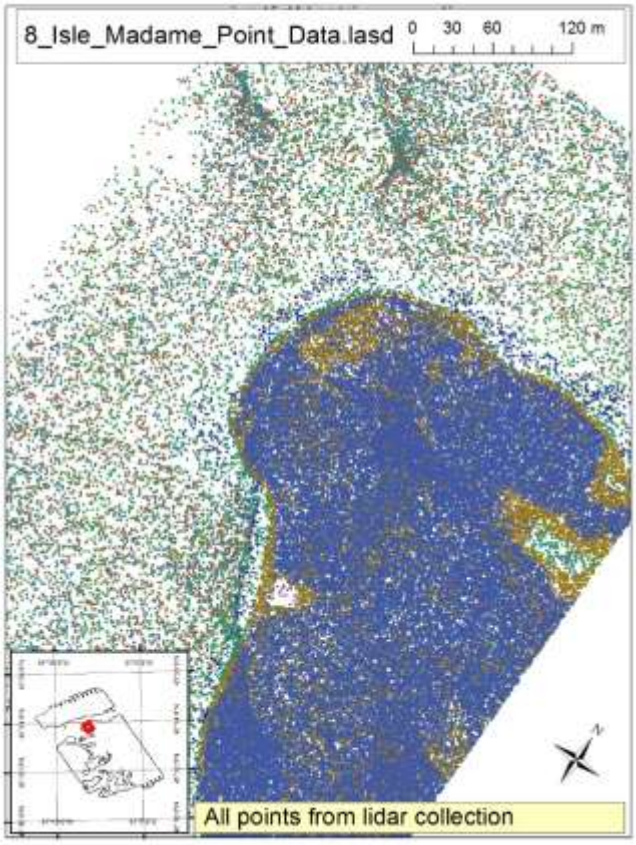

201503 ILSE MADAME > Grids

Orthomosaics

Aerial photography orthomosaics are delivered in georeferenced .TIFF format, and similarly projected in NAD 83 UTM zone 20N in two separate products; one at a 20 cm ground spatial resolution – and one at 5 cm. Both data contain 4 bands; Red, Green, Blue, and Near Infrared.

Report

The accompanying report can be found in the supplied external drive as a .PDF format.

Shoreline Classification

Shoreline classification products and accompanying data as described in the accompanying report has been provided including; single frame aerial photographs, small segments of manually color balanced aerial photograph orthomosaics, and a preliminary test case of shoreline substrate type classification results (in both a raster and polygon product).

Preliminary shoreline substrate classification codes used for raster and polygon products are as follows:

4	Sea vegetation
9	Submerged Gravels
15	Loose Gravels
21	Fine Gravels
22	Shore Grasses
23	Tightly Consolidated Fine Sediment
24	Steep Glacial Till Bank
25	Tightly Packed Sands
26	Shallow Till Bank
27	Very Tightly Packed Fine Sediment
28	Loose Cobbles-Boulders

Accessing the Data

Other than on the external drive as provided, it is possible data can be supplied via FTP if specifically requested.

Data Use

The Applied Geomatics Research Group of the Nova Scotia Community College maintains full ownership of all data collected by equipment owned by NSCC and agrees to provide the end user who commissions the data collection a license to use the data for the purpose they were collected for upon written consent by AGRG-NSCC. The end user may make unlimited copies of the data for internal use; derive products from the data, release graphics and hardcopy with the copyright acknowledgement of “Data acquired and processed by the Applied Geomatics Research Group, NSCC”. Data acquired using this technology and the intellectual property (IP) associated with processing these data are owned by AGRG/NSCC and data will not be shared without permission of AGRG/NSCC.

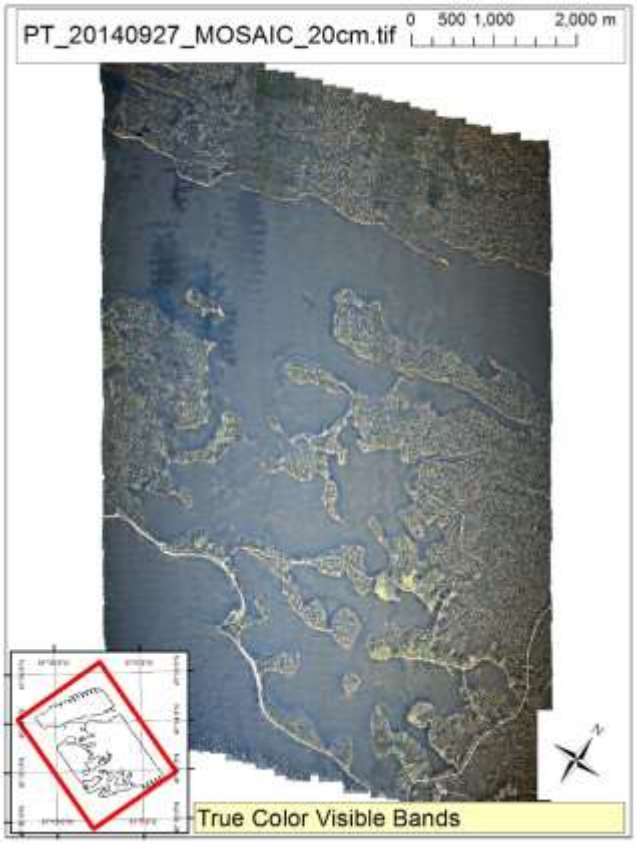

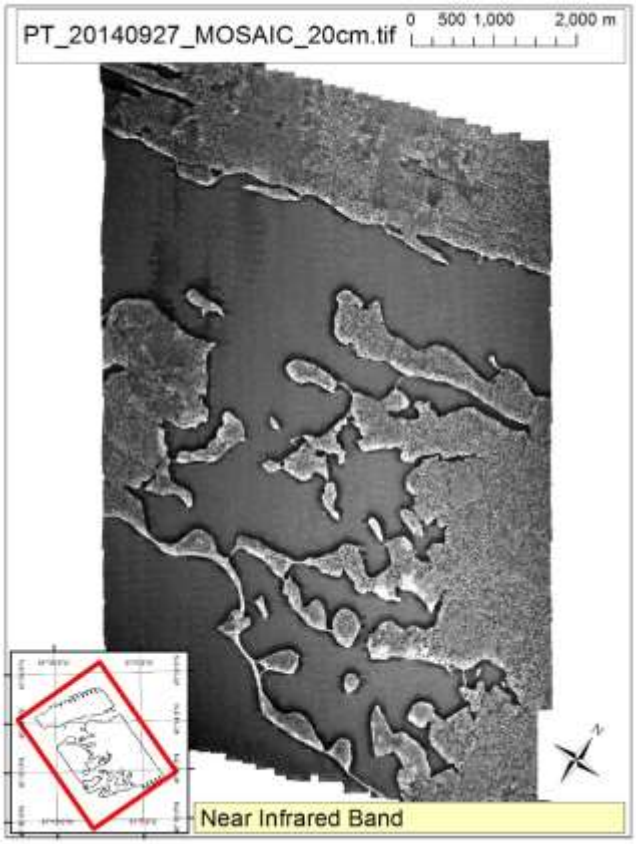

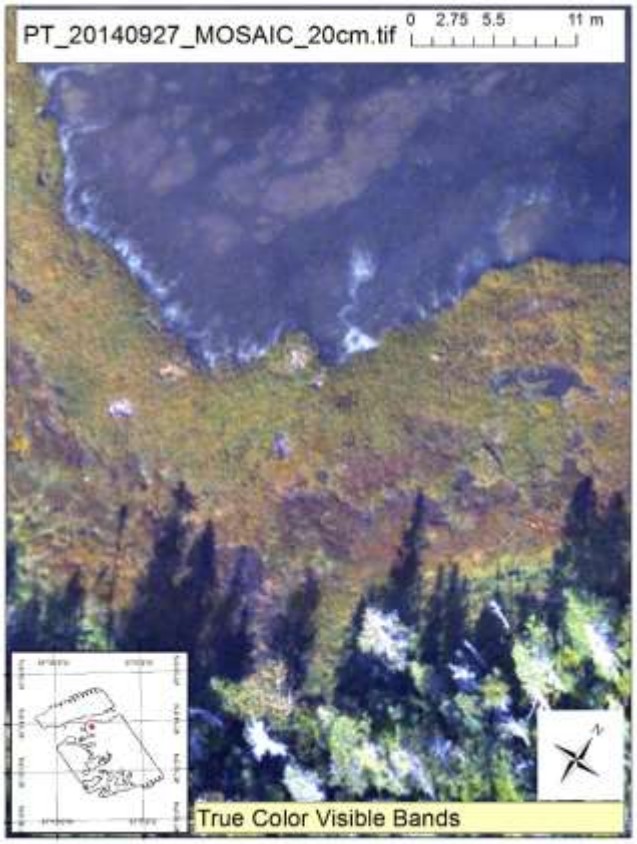

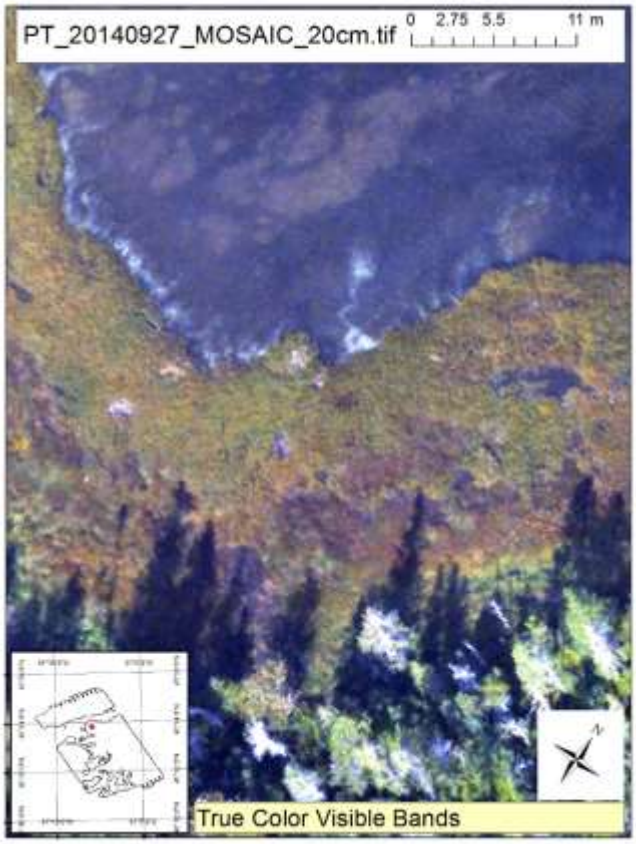

201503 ILSE MADAME > Orthomosaics

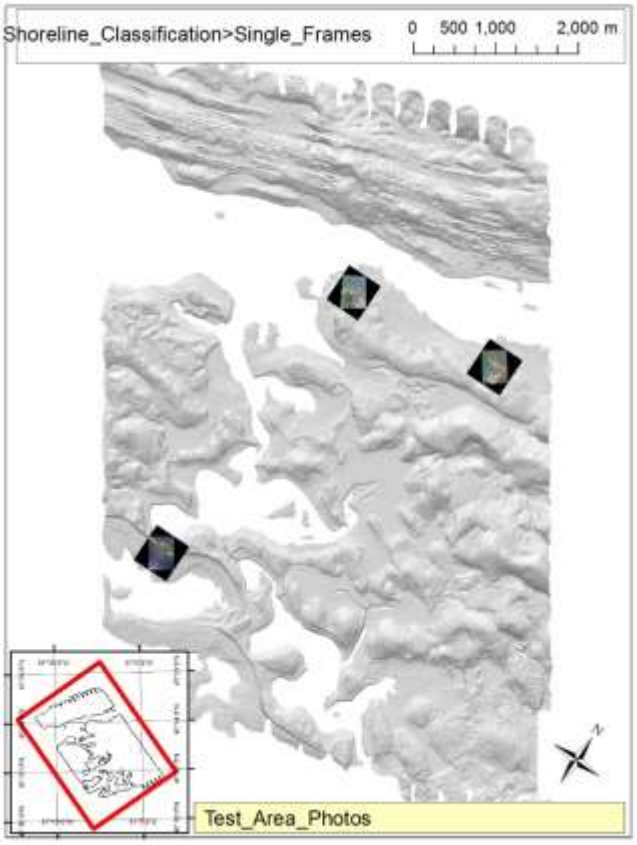

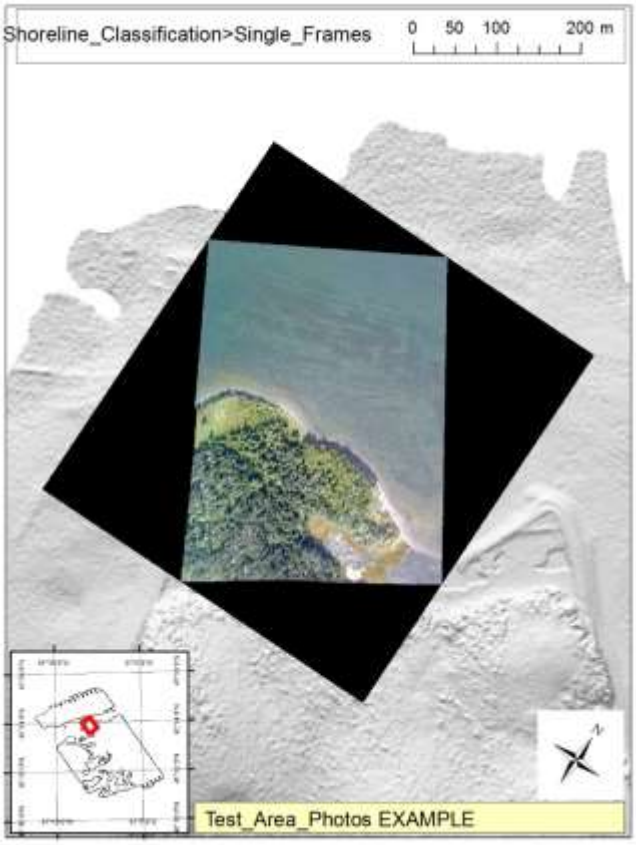

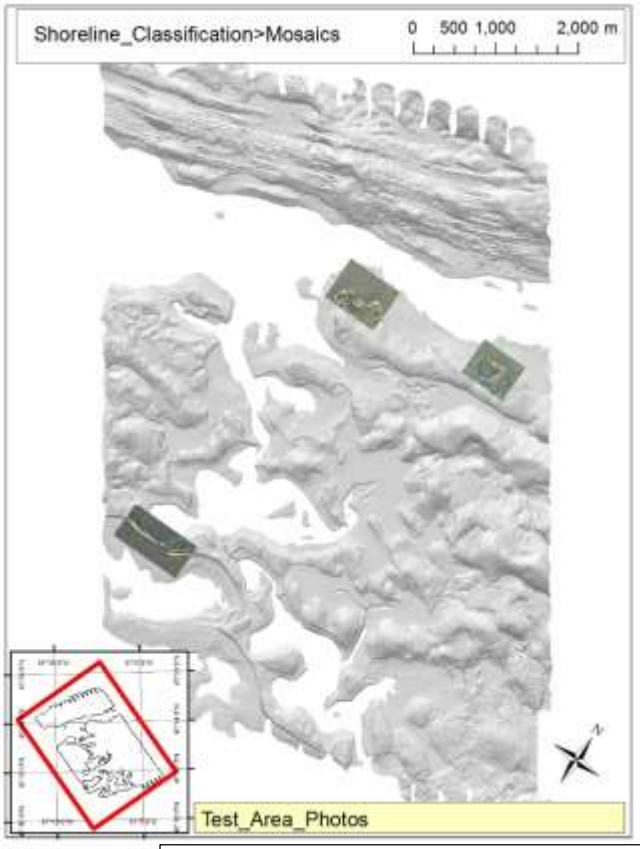

201503 ILSE MADAME > Shoreline Classification

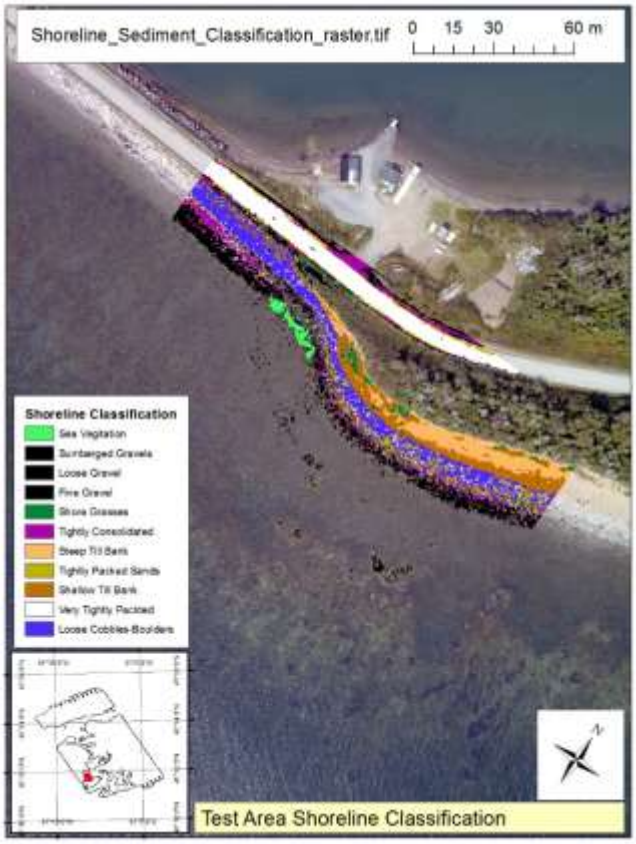

201503 ILSE MADAME > Shoreline Classification